J. Paleont., 81(6), 2007, pp. 1168–1193

0022-3360/07/0081-1168$03.00

ONTOGENY AND EVOLUTION OF THE EARLY CAMBRIAN TRILOBITE GENUS *NEPHROLENELLUS* (OLENELLOIDEA)

MARK WEBSTER

Department of the Geophysical Sciences, University of Chicago, 5734 South Ellis Avenue, Chicago, IL 60637, <mwebster@geosci.uchicago.edu>

ABSTRACT—The cephalon of *Nephrolenellus multinodus* and its stratigraphically higher sister-taxon *N. geniculatus* passed through the same four successive phases of development: entry into phase 2 is defined by a change from a decrease to an increase in the dynamic pattern of distance between the intergenal spine bases relative to cephalic length; entry into phase 3 is defined by the appearance of genal spines; and entry into phase 4 is defined by the effective isolation of glabellar furrow S3 from the axial furrow. Phase transitions were associated with significant changes in allometric growth patterns of the cephalon. Five instars are identified within the early development (phases 1 and 2) of *N. multinodus*. Despite the general similarity in cephalic ontogeny, significant interspecific differences in patterns of shape change are documented throughout phases 1, 2, and 3 of cephalic development which, with differences in rates of glabellar shape change relative to size (higher in *N. multinodus*) and ontogenetic loss of glabellar axial nodes (higher in *N. geniculatus*), demonstrate that evolutionary modification to ontogeny was mosaic and complex. Stratigraphic occurrences and a temporal trend towards increased rate of glabellar axial node loss relative to size in *N. geniculatus* are consistent with a hypothesis that *N. geniculatus* was a direct descendant of *N. multinodus*. However, ontogenetic data are needed for immediate outgroups of *Nephrolenellus* to determine whether two potential autapomorphies of *N. multinodus*, which refute such a hypothesis, are indeed unique to this taxon. *Nephrolenellus jasperensis* is recognized as a junior synonym of *N. multinodus*.

INTRODUCTION

THE OLENELLOIDEA Walcott, 1890 is a significant monophyletic group (Lieberman, 1998, 2001) of Lower Cambrian redlichiid trilobites. The diversity and abundance of olenelloid fossils render them ideal for biostratigraphy, and a detailed understanding of olenelloid phylogeny and paleobiology is central to several key evolutionary issues, including resolution of the controversial early evolutionary history of the Trilobita Walch, 1771 (Lauterbach, 1983; Fortey and Whittington, 1989; Whittington, 1989; Ramsköld and Edgecombe, 1991; Fortey and Owens, 1997; Fortey, 2001; Lieberman, 1998, 2001, 2002; Jell, 2003; Paterson and Edgecombe, 2006), and analysis of rates and modes of evolution during the Early Cambrian, a critical interval in metazoan history.

Nephrolenellus Palmer and Repina, 1993 is an important genus of olenelloid trilobite: it serves as a useful biostratigraphic marker for uppermost Dyeran strata (Palmer and Halley, 1979; Palmer, 1998; Fowler, 1999; Sundberg and McCollum, 2000; Webster et al., 2003; Webster, 2003, 2005; Fig. 1); it has been included in recent broad-scale cladistic analyses of early trilobites (Lieberman, 1998; Paterson and Edgecombe, 2006); and it has been used in quantitative studies of the effect of compaction on fossil morphology (Webster and Hughes, 1999) and the nature of evolutionary modifications to ontogeny (Webster et al., 2001; Webster and Zelditch, 2005). Specimens assigned to the two constituent species, *N. multinodus* Palmer in Palmer and Halley, 1979 and *N. geniculatus* Palmer, 1998, are known from the Great Basin of California, Nevada, and Arizona (Fig. 1), and from a single occurrence in Canada (designated a new species by Lieberman, 1999, but here formally re-synonymized with *N. multinodus*). The genus is demonstrably monophyletic (Webster et al., 2001). Although silicified material of the *Nephrolenellus* species from the Great Basin has been used extensively in the recent literature (Palmer, 1998; Webster and Hughes, 1999; Webster et al., 2001; Webster and Zelditch, 2005), formal description and detailed photographic documentation of their respective ontogenies has not yet been published.

This paper provides a detailed description of the ontogeny of *Nephrolenellus multinodus* and of *N. geniculatus*, including an expanded description of their mature morphology based on larger sample sizes than were available at the time of their original descriptions. The mature thorax of *N. multinodus* is described and figured for the first time. Instars are identified within the early ontogeny of *N. multinodus* based on cephalic morphology alone, representing only the second olenelloid species for which discrete early molt stages have been unambiguously recognized. The patterns of ontogenetic cephalic shape change followed by each species are graphically depicted and quantitatively investigated using geometric morphometric techniques, expanding upon and slightly revising some aspects of previous studies (Webster et al., 2001; Webster and Zelditch, 2005). The study provides detailed documentation of the nature of the morphological differences between *N. multinodus* and its sister-taxon *N. geniculatus*, and how those differences arose during ontogeny. The possibility that *N. multinodus* was directly ancestral to *N. geniculatus*, with implications that the interspecific differences equate directly to evolutionary modifications of ontogeny within an anagenetic lineage, is discussed, but unequivocal resolution of this issue will require additional data in closely related outgroup taxa.

SUBDIVISIONS OF CEPHALIC DEVELOPMENT IN *NEPHROLENELLUS*

Phases of cephalic development.—Trilobite ontogeny is traditionally subdivided into the protaspid, meraspid, and holaspid periods (Beecher, 1895; Raw, 1925; reviewed by Chatterton and Speyer, 1997), based on the nature of trunk articulation. The silicified *Nephrolenellus* material described here is invariably disarticulated, and knowledge of early ontogeny is restricted to cephalic morphology alone. Assignment of *Nephrolenellus* specimens to particular stages of the traditional ontogenetic scheme is therefore impossible. However, four successive phases of cephalic development have been recognized within the ontogeny of both *Nephrolenellus* species (Webster et al., 2001; Webster and Zelditch, 2005; explained in detail for the first time below), and these phases offer an alternative scheme by which the ontogeny of the species may be subdivided in the absence of thoracic information. The four phases are deemed to be homologous in both *Nephrolenellus* species, as evinced by the conserved order of phase-defining events and by the similar cephalic sizes at which the phase transitions occurred. The pattern of cephalic shape change followed as a function of size (i.e., the nature of allometric growth) can be demonstrated to undergo a significant shift at each phase transition where preservation permits quantitative analysis (see below). Specific rates and patterns of morphological development of the cephalon can be meaningfully compared between the taxa in the same phase of cephalic development (Webster et al., 2001; Webster and Zelditch, 2005; below).

The earliest preserved portion of the ontogeny of the *Nephrolenellus* cephalon is divided into two phases, distinguished from each other by the dynamic pattern of distance between the intergenal spine bases relative to sagittal cephalic length: this ratio initially decreases (phase 1), then increases (phase 2) as a function of cephalic length (Fig. 2.1, 2.2). The phase 1 to phase 2 transition occurs at sagittal cephalic length of approximately 0.63 mm in *N. multinodus* and 0.72 mm in *N. geniculatus*. Entry into phase 3 of

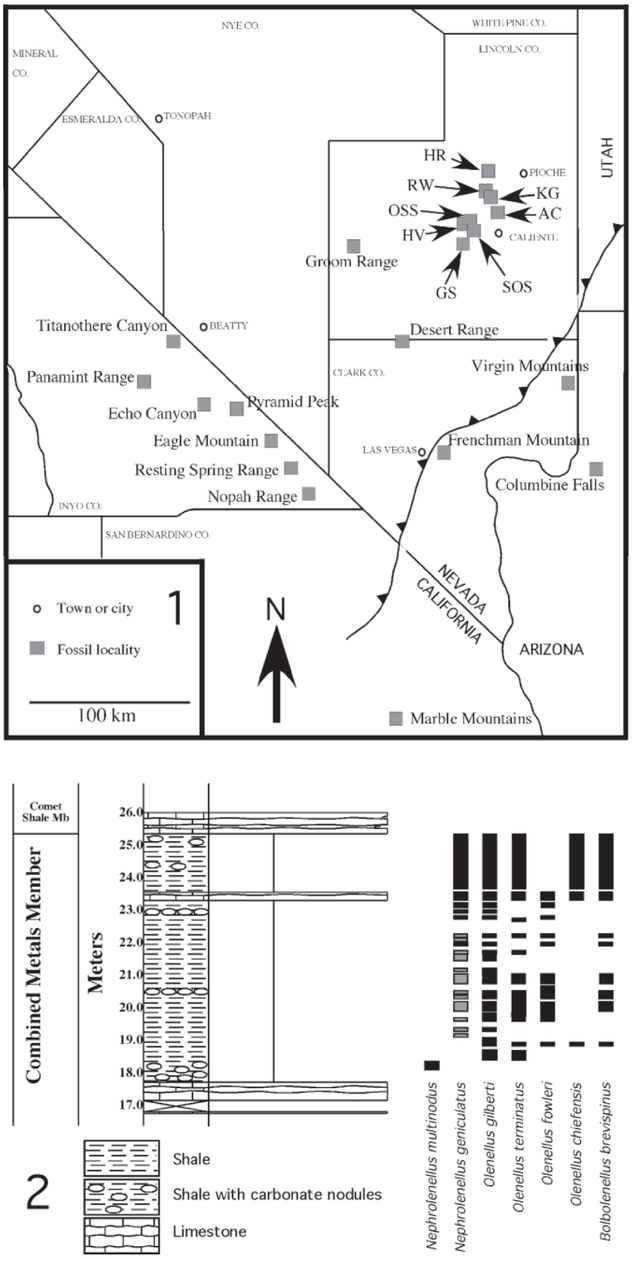

FIGURE *1—1*, Map of localities in the Great Basin from which *Nephrolenellus* specimens have been recovered. Abbreviations: AC, Antelope Canyon; GS, Grassy Spring; HR, Highland Range; HV, Hidden Valley; KG, Klondike Gap; OSS, Oak Spring Summit; RW, Ruin Wash; SOS, Seven Oaks Spring. See text for stratigraphic details. The black line with triangles marks the eastern edge of Mesozoic thrusting (overthrust block to west). *2*, Occurrences of common olenelloid trilobites in the uppermost Dyeran portion of the Pioche Formation at the Hidden Valley section, Burnt Springs Range, Nevada. Meterage refers to distance above base of Combined Metals Member. The limestone marking the base of the Comet Shale Member contains basal Delamaran trilobites. Black boxes indicate stratigraphic levels at which species were recovered. Grey boxes indicate stratigraphic levels at which samples of *Nephrolenellus geniculatus* are dominated by morphologically mature specimens retaining an axial node on glabellar lobe L1 and often L2 in addition to the axial node on LO. See text for details.

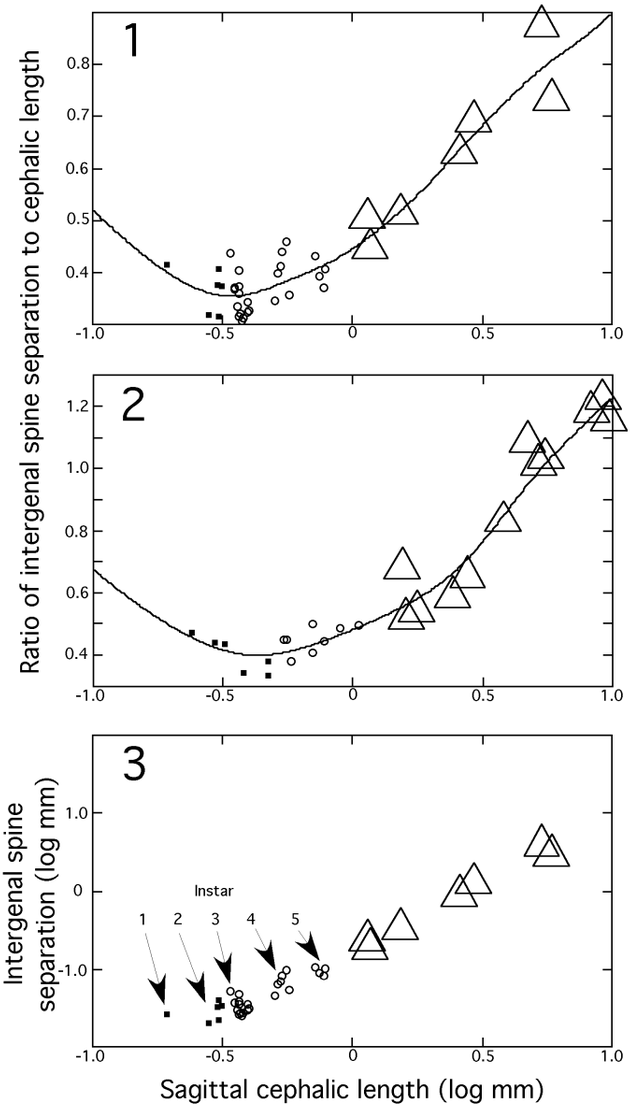

FIGURE *2—1, 2,* Transverse distance between adaxial margins of intergenal spine bases relative to sagittal cephalic length, showing shift from decreasing to increasing ratio marking the transition from phase 1 into phase 2 of cephalic development in both *Nephrolenellus multinodus* (1) and *N. geniculatus* (2). Plots have been fitted with a distance weighted least squares regression function (McLain, 1974) for illustrative purpose only. *3*, Instars revealed by data clustering in a plot of transverse distance between adaxial margins of intergenal spine bases against sagittal cephalic length for *N. multinodus*. Phase 1 of cephalic development consists of two instars, and phase 2 consists of three. Symbols in all plots: squares, phase 1 of cephalic development; circles, phase 2 of cephalic development; triangles, early phase 3 of cephalic development.

cephalic development is defined as the point at which the genal spines first appear. Absent through phases 1 and 2 of cephalic development, the genal spines are first seen as tiny, ventrolaterally-projecting nubbins, located immediately adjacent to the abaxial margin of the intergenal spine bases (Figs. 8.17, 8.18, 8.21, 15.13). They are often obscured from dorsal view on account of their slightly ventral aspect. Entry into phase 3 of cephalic development occurs at sagittal cephalic length of approximately 1.03 mm in both species. Considerable change in cephalic outline occurred during phase 3, as the posterior cephalic border between the axial furrow and the intergenal spines and between the intergenal and genal spines underwent dramatic relative elongation.

Entry into phase 4 of cephalic development is defined by the effective isolation of the third glabellar furrow (S3) from the axial furrow (Figs. 9.14, 16.1, 16.4, 16.7) and occurs at sagittal cephalic length of approximately 3.1 mm in both species. Effective isolation of S3 as a pit-like dimple resulted from lateral expansion of the third glabellar lobe L3 relative to lobes L2 and the frontal glabellar lobe LA: the anterolateral margins of L3 show a proportionally increasing extent of contact and ultimate merger with the posterior margins of LA and the ocular lobes as a function of cephalic size (compare Fig. 9.1, 9.13, 9.14, and 9.19; and Figs. 15.19, 15.23, 15.26, 16.1, 16.4, and 16.7). The typical mature outline of the *Nephrolenellus* glabella, narrowest (tr.) at L2 and with progressive anterior shortening (sag.) of L1 to L3, is attained on phase 4 cephala.

Instar recognition.—Size increase and shape change during trilobite ontogeny was restricted to brief molt periods following ecdysis of the old exoskeleton and prior to hardening (sclerotization and mineralization) of the new one. Distinct instars, representing the intermolt stages of fixed morphology, have been recognized in trilobites based on patterns of release of trunk segments into the thorax and by distinct size-clustering of conspecific cephala (reviewed by Chatterton and Speyer, 1997). Prior to the present study, instars had been unambiguously identified in only one olenelloid species: *Olenellus puertoblancoensis* (Lochman, 1952)(see Palmer, 1957; misidentified as *Paedeumias clarki* Resser, 1928). (Purported instars in *Mesolenellus hyperborea* [Poulsen, 1974] detected through measures of cephalic dimensions [see Poulsen, 1974] have recently been cast into doubt by statistical investigation [Hunt and Chapman, 2001].)

Prior to differentiation of the genal spines, distinct clusters of *Nephrolenellus multinodus* cephala can be recognized based on the relationship between the separation of the intergenal spine bases and cephalic length (Fig. 2.3). Although sample size is small, these clusters are tentatively interpreted as instars. Two instars can be recognized within phase 1 of cephalic development, and three within phase 2. Dyar's coefficient for proportional change in sagittal cephalic length between successive instars averages a biologically reasonable 1.16 (range 1.09 to 1.21). Palmer (1957) also recognized five instars prior to differentiation of the genal spines in *Olenellus puertoblancoensis*, and also calculated an average Dyar's coefficient of 1.16. Assuming homology of the five pre-phase 3 instars identified in *N. multinodus* and *O. puertoblancoensis*, phases 1 and 2 of cephalic development in *Nephrolenellus* (as defined here) equate precisely to stages I and II, respectively, of cephalic development in *O. puertoblancoensis* (as defined by Palmer, 1957; discussed below).

Based on the present sample size, putative instar clusters could not be identified among small cephala of *Nephrolenellus geniculatus*. However, entry into phases 2 and 3 occur at similar cephalic lengths, and the relationship between separation of the intergenal spines and cephalic length is consistent in both *Nephrolenellus* species (Fig. 2.1, 2.2). It is therefore possible that *N. geniculatus* passed through the same number of molts prior to differentiation of the genal spines.

Relationship of the phases to previous models of trilobite ontogeny.—The precise relationship between the four phases of cephalic development in *Nephrolenellus* and the traditional subdivisions of trilobite ontogeny (see above) is unknown. Phase 1 cephala are undoubtedly post-protaspid, possessing the posterior cephalic margin along which the transitory pygidium or first thoracic segment would have articulated (Figs. 8.1, 15.1, 15.2). (Indeed, protaspides have never been recovered for any olenelloid species despite intensive searching, and were apparently unmineralized in life [Fortey and Whittington, 1989; Whittington, 1989]). The smallest *Nephrolenellus* cephala in phase 1 of development are comparable in size to degree 0 meraspides of other trilobites (sagittal cephalic length 0.49 mm; see Chatterton and Speyer, 1997). No totally complete *Nephrolenellus* specimens (of any size) are known, rendering the meraspid/holaspid transition impossible to identify.

Alternative subdivisions of olenelloid ontogeny based solely on cephalic development have been previously proposed (Tasch, 1952; Palmer, 1957; McNamara, 1986; a scheme similar to that of Palmer [1957] but of broader scope was presented by Bohach [1997], but this remains unpublished and will not be discussed here). None of these schemes were based on observations of *Nephrolenellus*, and their application to the ontogeny of this genus meets with only limited success.

Palmer (1957) documented in detail the ontogeny of *Olenellus fowleri* Palmer, 1998 (misidentifed as *O. gilberti* Meek in White, 1874) and *O. puertoblancoensis*, and defined five successive stages of cephalic development, numbered I (developmentally youngest) to V. The stage I to stage II transition was defined by Palmer (1957) as the first instar on which the posterior tip of the ocular lobe is well defined and distinct from the posterior ocular line (which runs from the ocular lobe onto the intergenal spine). Entry into stage III was indicated by the first appearance of the genal spines. Stage IV was defined by the disappearance of the procranidial spines, and stage V by reduction of the intergenal spines to nubs. The same stages could be applied (in at least some aspects) to several other olenelloids, leading Palmer (1957, p. 121) to suggest that his scheme was representative of most taxa. Certainly, entry into Palmer's (1957) stage III equates directly to entry into phase 3 as defined here. Phases 1 and 2 as defined here equate to Palmer's (1957) stages I and II based on commonality of instar numbers (see above), although the transition-defining events are different (the posterior tips of the ocular lobes are well defined from the earliest preserved ontogenetic stages in *Nephrolenellus*; see Figs. 8.1, 15.1, 15.2). Palmer's (1957) stage III to stage IV transition is applicable only to species which initially developed procranidial spines, although such spines are now recognized to be of limited phylogenetic distribution within the Olenelloidea (and are absent in *Nephrolenellus*, contra Paterson and Edgecombe [2006, character 42]). Entry into Palmer's (1957) stage V is somewhat subjective and arbitrary, as genal spines progressively increased and intergenal spines progressively decreased in length during phases 3 and 4 of cephalic development. It is also difficult to apply to taxa retaining distinct intergenal spines at morphological maturity. Nevertheless, the intergenal spines are expressed as small nodes or spines on *Nephrolenellus* cephala in late phase 3 as defined here (Figs. 9.13, 15.30).

Tasch (1952) proposed four successive stages of cephalic development in olenelloids, based on ontogenetic changes in the nature of contact between the ocular lobes and LA. However, the pattern of ontogenetic ocular lobe differentiation followed by *Elliptocephala asaphoides* Emmons, 1844, used as a standard in Tasch's (1952) scheme, is not representative of olenelloids in general (personal observation) or of *Nephrolenellus* in particular. Thus, although based on the development of a morphological feature present in all olenelloids, Tasch's (1952) ontogenetic subdivisions are not widely applicable.

McNamara (1986) implied that the glabella followed a generally conserved pattern of development among all Cambrian trilobites, including olenelloids. Five successive stages of glabella development were defined, based on changes in the morphology of glabellar lobes and furrows and in the relative size of the preglabellar field. In the earliest *stasis* stage, the anterior margin of LA was in direct contact with the anterior cephalic border. The glabella was parallel-sided, glabellar lobes roughly equidimensional, and glabellar furrows transverse. This stage was equated to the protaspid (and in some taxa, the early meraspid) period (McNamara, 1986). In the subsequent *retraction* stage, the anterior border migrated away from the anterior margin of LA and a preglabellar field developed. LA was diagrammatically shown to be wider (tr.) than more posterior lobes (McNamara, 1986, fig. 5b), suggesting that LA was proportionally laterally expanding

during this stage. Due to the relative posterior migration of LA, glabellar furrows became reoriented posteriorly adaxially. This stage was equated to the early meraspid period. In the following *protraction* stage (late meraspid to early holaspid), LA proportionally expanded in an anterior direction, causing a relative shortening (and sometimes loss) of the preglabellar field. In the *expansion* stage, LA continued to proportionally expand laterally and/or anteriorly following contact with the anterior cephalic border. This relative inflation of LA could be extrapolated into the final *development* stage, in which the glabella became proportionally greatly enlarged and glabellar furrows often became effaced. McNamara's (1986) scheme is based on (and relates only to) the development of the glabella and its relationship to the anterior cephalic border. It is likely that phase 1 in *Nephrolenellus* (herein) represents at least in part the stasis stage of McNamara (1986), and phases 2 through 4 perhaps represent the retraction, protraction, and expansion stages. However, McNamara's (1986) stages (in particular the retraction stage) are defined in part by reference to the relative size of the preglabellar field, rendering parts of his scheme difficult to apply to taxa lacking a preglabellar field throughout ontogeny (including *N. geniculatus*). Furthermore, the practical distinction between McNamara's (1986) protraction, expansion, and development stages seems to be somewhat arbitrary, rendering their precise application equivocal.

Attainment of morphological maturity in trilobites was sometimes associated with a shift in the pattern or rate of shape change relative to size increase (e.g., Hughes, 1994; Kim et al., 2002). Geometric morphometric analyses (detailed below) suggest that in both *Nephrolenellus* species the rate of glabellar shape change relative to size increased slightly upon entering phase 3 of cephalic development, but no obvious change is apparent in later stages of cephalic development in either species (Fig. 3; see also Webster and Zelditch [2005, fig. 5b] for a similar study involving a more comprehensive landmark coverage of cephalic morphology). However, the transition from phase 3 into phase 4 is roughly coincident with the upper size limit of well preserved silicified material and the lower size limit of well preserved material preserved in shale (Fig. 3), and quantification of the rate (and the pattern) of glabellar growth across this transition is potentially complicated by taphonomic overprint. The relative timing of attainment of morphological maturity (in any sense, including the traditional holaspid period) and sexual maturity in trilobites is unknown.

Although it is beyond the scope of the present paper to identify homologous phases in other olenelloid species, the four subdivisions of cephalic ontogeny for *Nephrolenellus* recognized herein are based on specific developmental events that appear to be more widely applicable in a phylogenetic sense. If such a generalization holds, then this scheme has advantages over others (e.g., Tasch, 1952; Palmer, 1957; McNamara, 1986) in that the stages are defined in terms of morphological structures developed on all olenelloids, and that the distinction between particular phases of development is less arbitrary. The broader applicability of the present scheme will be discussed in future work.

Quantitative analysis of ontogeny.—The burgeoning field of geometric morphometrics allows rigorous multivariate quantification of shape and shape change (Bookstein, 1991; Zelditch et al., 2004), and the elegance of the techniques is revolutionizing biometry. Geometric morphometrics offers a powerful toolkit for answering paleobiological questions, and the methods have already been employed in several trilobite studies (Hughes and Chapman, 1995; Smith, 1998a, b; Hughes et al., 1999; McCormick and Fortey, 1999, 2002; Smith and Lieberman, 1999; Webster and Hughes, 1999; Webster et al., 2001; Kim et al., 2002; Clausen, 2004; Crônier et al., 2004; Fusco et al., 2004; Adrain, 2005; Webster and Zelditch, 2005; Crônier and Fortey, 2006; Adrain and Westrop, 2006). Such morphometric methods are used here to demonstrate the significance of modifications to patterns of shape change upon entry into particular phases of development, and to further demonstrate the utility of morphometric techniques in detailed ontogenetic studies.

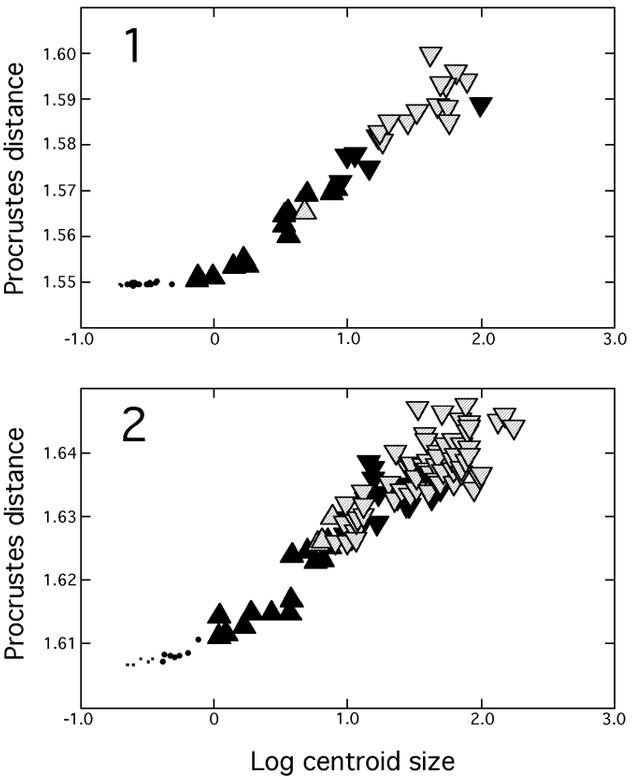

FIGURE *3*—Rate of glabellar shape change relative to size in *Nephrolenellus multinodus* (1; n = 56) and *N. geniculatus* (2; n = 107), using landmark configuration 4 (Fig. 4). Shape change is quantified as partial Procrustes distance from a designated reference form (the consensus of all specimens assigned to the second instar in phase 1 of cephalic development for *N. multinodus*, the consensus of the two smallest specimens in phase 1 of cephalic development for *N. geniculatus*). Size of a specimen is quantified as the natural log of the centroid size of its landmark configuration (i.e., the square root of the sum of squared distances between each landmark and the centroid of the configuration; Bookstein, 1991). Symbols in both plots: squares, phase 1 of cephalic development; circles, phase 2 of cephalic development; upward-pointing triangles, phase 3 of cephalic development; downward-pointing triangles, phase 4 of cephalic development; solid shading, landmark data extracted from noncompacted specimens (preserved in a silicified state or in limestone); hatched shading, landmark data extracted from internal molds of taphonomically compacted specimens preserved in shale. See text for details.

Cephalic shape is summarized by digitizing the x, y coordinates of a series of discrete points (landmarks) on the sclerite, recognizable and homologous on all specimens included within a given analysis (Fig. 4). Superimposition of landmark configurations of different specimens (translated, rotated, and rescaled according to a specified optimality criterion, e.g., generalized least-squares [GLS] Procrustes methods [Bookstein, 1991; Dryden and Mardia, 1998]) then permits differences in cephalic shape between those specimens to be investigated. Measurement error is negligible: repeated digitizing of specimens demonstrated that within-specimen measurement error is two orders of magnitude smaller than morphological variation among similar sized, conspecific specimens. Specimens showing evidence of tectonic distortion (e.g., Figs. 5.2, 5.4, 5.13, 7) or otherwise poor preservation were omitted from morphometric analysis.

The amount of shape difference between the configurations of any two specimens is quantified as a partial Procrustes distance

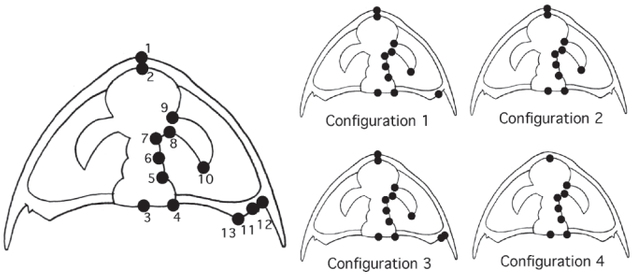

FIGURE 4—Landmarks selected for morphometric analysis of the ontogeny of the two *Nephrolenellus* species. Landmarks are shown only on the right side of the cephalon for clarity: coordinates of landmarks on the left side were also digitized, and were computationally reflected across the sagittal axis and averaged with the homologous landmark on the right side to reduce data redundancy. Left, the full set of 13 landmarks, representing maximal shape summary of cephala in phase 4 of development (as utilized by Webster et al., 2001). Landmarks are defined as follows: 1, anteriormost point of cephalon on sagittal axis; 2, anteriormost point of glabella on sagittal axis; 3, midpoint of posterior margin of occipital ring (LO) on sagittal axis; 4, juncture of axial furrow with posterior cephalic margin; 5, juncture of axial furrow with occipital furrow (SO); 6, juncture of axial furrow with S1; 7, juncture of axial furrow with S2; 8, juncture of axial furrow with S3; 9, juncture of axial furrow with anterior margin of ocular lobe; 10, posterior tip of ocular lobe; 11, base of intergenal spine (adaxial side); 12, base of genal spine (adaxial side); 13, adgenal angle. Right, four configurations based on subsets of the 13 landmarks, appropriate for analysis of patterns of shape change over different portions of ontogeny. Configuration 1, 11 landmarks representing maximal shape summary of cephala in phases 1 and 2 of development (which lack an adgenal angle and genal spines); configuration 2, 10 landmarks; configuration 3, 12 landmarks representing maximal shape summary of all cephala in phase 3 of development; configuration 4, 8 landmarks representing maximal summary of glabellar shape through all phases of cephalic development.

(the square root of the summed squared distances between homologous landmarks on the two configurations following GLS partial Procrustes superimposition; Bookstein, 1991). Plots of partial Procrustes distance of conspecific individuals of different size (developmental age) away from a designated reference specimen in an early developmental stage versus size therefore reveal the ''developmental rate'' (as a function of size) during ontogeny (Fig. 3). (The relationship between developmental rate as a function of size and developmental rate as a function of true [chronological] time is of course unknown in trilobites.)

Ontogenetic shape change can be quantified as a multidimensional vector describing shape differences between superimposed landmark configurations of conspecific individuals of different size. Each component of the vector represents a pattern of landmark offset between superimposed landmark configurations (the regression coefficients of shape [shape coordinates or warp scores] on size, normalized to unit length). Modification to patterns of shape change during ontogeny (ontogenetic allometric repatterning) can be assessed by calculating an angle between vectors of shape change for successive phases of ontogeny (the arccosine of the dot product of the normalized ontogenetic vectors: see Webster et al., 2001; Zelditch et al., 2004). A statistically significant angle between successive phases of ontogeny (compared to the range of angles expressed within each phase, assessed by bootstrap resampling; Webster et al., 2001; Zelditch et al., 2003; Zelditch et al., 2004) indicates that the pattern of growth followed by the species differed between the phases. In the analyses presented below, vectors of shape change were calculated from shape coordinates (following superimposition using Bookstein registration) and from warp scores generated through thin-plate spline analysis (TPS) of configurations, as discussed and previously utilized by Webster et al. (2001). Results of all analyses were robust to changes in designated baseline landmarks (for vectors derived from Bookstein coordinates) and reference form (for vectors derived from warp scores). Morphometric analyses were conducted using software in the Integrated Morphometrics Programs (IMP) package, compiled by H. D. Sheets in Matlab6 (Mathworks, 2000) and freely available electronically at http://www.canisius.edu/~sheets/morphsoft.html (see also Zelditch et al., 2004).

Morphospace distortion introduced by projecting data from non-linear shape space into a linear tangent plane for statistical analysis is negligible: for *Nephrolenellus geniculatus* data (landmark configuration 4, silicified plus non-silicified specimens, n = 111) the correlation between partial Procrustes distance and distance in the tangent-plane is strong (0.999997) with a slope of 0.997 (calculated using the program tpsSmall, available at http://life.bio.sunysb.edu/morph/).

Quantification of rates and patterns of ontogenetic shape change requires well preserved material. Taphonomic compaction affects fossil morphology in the horizontal as well as vertical plane and this can inflate estimates of shape variability (e.g., Webster and Hughes, 1999) and modify the patterns of shape change detected. Ideally, noncompacted specimens (preserved in limestone or in a silicified state) should be used for detailed morphometric investigation. However, preservation of large (phase 4), intact cephala in a silicified state is rare in the Lower Cambrian deposits examined to date (see Fig. 3). The present analyses of rates and patterns of ontogenetic shape change were conducted on silicified material, supplemented by well preserved but taphonomically compacted cephala in phase 4 of development preserved in shale where noted.

Analyses presented here are based on a larger sample size (Appendix, accessed in the Supplemental Data Archive at www.journalofpaleontology.org) than was available in previous studies (Webster et al., 2001; Webster and Zelditch, 2005) and expand upon (and slightly revise some aspects of) the previous results. These new analyses allow a more detailed understanding of the early portion of ontogeny (phases 1 and 2 of cephalic development) in particular.

SYSTEMATIC PALEONTOLOGY

Terminology.—Morphological terminology largely follows that of Whittington and Kelly (1997), with modifications to thoracic terminology proposed by Palmer (1998). However, olenelloid ontogeny reveals that the term ''intergenal angle'' (as presently defined; a deflection or kink in the posterior cephalic border) is in need of refinement, as it has been used to describe two non-homologous anatomical features (see also Palmer, 1998). A revised terminology is proposed below to remove this ambiguity.

Subsequent to its initial differentiation, the genal spine became separated from the intergenal spine by elongation of the cephalic border between them. The posterior cephalic border was often deflected anterolaterally at the base of the intergenal spine so that the genal spine base was ''advanced'' relative to the intergenal spine base (Figs. 9.1, 9.5, 15.12, 15.16). The point of deflection of the posterior border at the base of the intergenal spine is here referred to as the *intergenal angle* (restricted definition). Later during ontogeny of many olenelloids, the posterior cephalic margin developed another distinct anterior deflection adaxial to the base of the intergenal spine (and to the intergenal angle) (Figs. 9.14, 9.18, 15.19, 15.26). This is here termed the *adgenal angle*. During subsequent growth the intergenal angle typically decreased in severity and the adgenal angle increased in distinctness (compare Figs. 9.22 and 9.25 or 15.26, 16.10, and 17.8). The intergenal angle was lost altogether in late ontogenetic stages of some taxa. Articulated specimens reveal that the adgenal angle closely approximates the distal limit of the articulation between the cephalon and first thoracic segment (T1). The term ''intergenal angle'' previously referred to any deflection in the posterior cephalic margin, and therefore failed to discriminate between the intergenal angle (restricted definition) and the adgenal angle (as defined here).

Materials.—Specimens listed below are housed in the Cincinnati Museum Center (CMCP), Denver Museum of Natural History (DMNH), the Field Museum, Chicago (FMNH), the Geological Survey of Canada, Ottawa (GSC), the Institute for Cambrian Studies, University of Chicago (ICS), the Museum of Comparative Zoology, Harvard (MCZ), the University of California, Riverside (UCR), the Smithsonian Institution, Washington, D.C. (USNM), and Yale Peabody Museum (YPM). Stratigraphic information (such as distance from marker beds) following ICS and UCR numbers refers to collateral field descriptions deposited at those institutions.

Order REDLICHIIDA Richter, 1932
Suborder OLENELLINA Walcott, 1890
Superfamily OLENELLOIDEA Walcott, 1890
Family BICERATOPSIDAE Pack and Gayle, 1971
Genus NEPHROLENELLUS Palmer and Repina, 1993

Type species.—*Olenellus multinodus* Palmer in Palmer and Halley, 1979.

Other species.—*Nephrolenellus geniculatus* Palmer, 1998.

Diagnosis.—Biceratopsids of relatively small size (sagittal length of cephalon rarely exceeds 11 mm). Ocular lobes strongly divergent from glabella; line from posterior tip of ocular lobe to point where adaxial margin of ocular lobe contacts axial furrow of L3 forms approximately 45° angle with sagittal axis. Glabella hourglass-shaped, constricted at L2; S2 transverse or gently convex anteriorly; S3 pit-like, effectively isolated from axial furrow; summit of LA slightly higher than more posterior glabellar lobes. Genal spine longer than length (exsag.) of LO, base located at point of maximal cephalic width (tr.). Thirteen prothoracic segments; opisthothorax of at least 23 segments, lacking long axial spine on anteriormost.

Occurrence.—Uppermost Dyeran; U.S.A. (California, Nevada, ?Arizona; Fig. 1), Canada (Alberta).

Discussion.—Lieberman (1999) included the absence of extraocular genal caeca and possession of axial spines on LO, L1, L2, and L3 in the generic diagnosis. Neither observation consistently applies to morphologically mature specimens of either of the included species: axial nodes are progressively lost throughout ontogeny (see below, Figs. 8.1, 8.4, 8.18, 8.29, 9.1, 9.24, 15.1, 15.6, 15.19, 15.23, 15.26, 16.7, 16.10, 16.20, 16.24. 17.1, 17.13; also Webster and Zelditch, 2005, fig. 4), and extraocular genal caeca are present on some mature cephala (Figs. 5.8, 5.9, 5.18, 12.4). Both characters are therefore removed from the diagnosis. Palmer and Repina (1993, 1997) included presence of a short preglabellar field in the diagnosis. However, *N. geniculatus* lacked a preglabellar field at all ontogenetic stages, and the length of the preglabellar field decreased ontogenetically (and is absent on large cephala) in *N. multinodus* (Figs. 8.1, 8.22, 8.29, 8.30, 9.1, 9.9, 9.13, 9.14, 9.18, 9.21, 9.24, 5.2, 5.13, 5.16).

Webster et al. (2001) discussed the close affinity of the two *Nephrolenellus* species with a new species which they termed *Nephrolenellus*? n. sp. However, this new species differs from *N. multinodus* and *N. geniculatus* in features such as possession of a slit-like (rather than pit-like) S3, 14 (rather than 13) prothoracic segments, and a long axial spine on the anteriormost opisthothoracic segment. Distinctions of these kinds are typically used to discriminate olenelloid genera, and the new species is therefore excluded from *Nephrolenellus*. Along with two other new species, it is assigned to a new genus to be described elsewhere (Webster, in press). *Nephrolenellus* shares closest affinity to this new genus and to the poorly known genus *Arcuolenellus* Palmer and Repina, 1993.

NEPHROLENELLUS MULTINODUS
(Palmer in Palmer and Halley, 1979)
Figures 5, 6, 7, 8, 9

Olenellus multinodus PALMER *in* PALMER AND HALLEY, 1979 (part), pp. 17, 56, 58, 67, 68, 72–73, 74, pl. 4, figs. 1–6, 9 only [non pl. 4, figs. 7, 8 = *Nephrolenellus geniculatus*]; WAGGONER AND COLLINS, 1995, p. 8

Olenellid trilobite, undescribed genus NORFORD, 1962, pl. 1, fig. 3

Nephrolenellus multinodus PALMER AND REPINA, 1993, p. 24, fig. 4.6; PALMER AND REPINA, 1997, p. 411, fig. 258.4a; ? SUNDBERG AND MCCOLLUM, 1997 (part), p. 1068 [listed in biostratigraphic range chart—refers at least in part to *Nephrolenellus geniculatus*]; PALMER, 1998, p. 661, figs. 6.10, 6.14; LIEBERMAN, 1998 (part), pp. 60, 62, 66, 74 [includes some details of *N. geniculatus*]; LIEBERMAN, 1999 (part), pp. 129, 131, 132, 133, 134 [includes some details of *N. geniculatus*]; SMITH AND LIEBERMAN, 1999, p. 462; FOWLER, 1999, pp. 47, 48, 49, 50; SUNDBERG, 2000, p. 266, fig. 7a; ? SUNDBERG AND MCCOLLUM, 2000, p. 606 [listed as questionable occurrence in biostratigraphic range chart]; WEBSTER, SHEETS, AND HUGHES, 2001, pp. 106, 110–136, figs. 4.1, 4.2a–d; LIEBERMAN, 2002, p. 699; LIEBERMAN, 2003, p. 63; WEBSTER, SADLER, KOOSER, AND FOWLER, 2003, figs. 2, 9, 10 [listed in biostratigraphic range charts]; WEBSTER AND ZELDITCH, 2005, pp. 366–370, figs. 3–6.

Nephrolenellus jasperensis LIEBERMAN, 1999, pp. 3, 129, 131, 132–134, fig. 20.6; SMITH AND LIEBERMAN, 1999, p. 462; LIEBERMAN, 2002, p. 699; LIEBERMAN, 2003, p. 63

not Olenellus multinodus STITT AND CLARK, 1984, p. 149 [referring to PALMER AND HALLEY, 1979, pl. 4, figs. 7, 8 = *Nephrolenellus geniculatus*]

not Olenellus multinodus WHITTINGTON, 1989, pp. 131, 132, 133 [referring to PALMER AND HALLEY, 1979, pl. 4, fig. 7 = *N. geniculatus*]

Description (mature morphology).—Cephalon semicircular in outline; proximal portion of posterior cephalic margin angled slightly posteriorly away from axial furrow, distal portion flexing anteriorly by 25° to 45° relative to proximal portion at rounded adgenal angle located two-thirds of distance from axial furrow to base of genal spine. Greatest observed cephalic length approximately 11.5 mm (sag.). Genal spine slender, base opposite or posterior to LO; length just less than half cephalic length (sag.). Short, pointed intergenal spine located between adgenal angle and base of genal spine (closer to genal spine), length less than that of LO (exsag.). Cephalic border well defined by distinct cephalic border furrow which weakens posterolaterally on some specimens (Fig. 5.3); rounded dorsally anteriorly, flattens slightly towards base of genal spine; width of anterior border opposite junction of ocular lobes with LA approximately half length (exsag.) of LO; posterior border narrows adaxially. Preglabellar field very short, length (sag.) about one-fifth that of LO on cephala up to 8 mm long (sag.), decreasing through ontogeny, represented only by a broad anterior border furrow on larger specimens (Fig. 5.13, 5.16). Glabella hourglass-shaped, constricted at L2. Maximum width of LA wider (tr.) than basal glabellar width. Posterior margin of glabella typically gently convex posteriorly, axial portion occasionally linear (tr.; Figs. 5.2, 5.10, 9.19). SO deep only abaxially, abaxial end slightly anterior to adaxial end. S1 deepest abaxially, oriented strongly anterolaterally abaxially. LO and L1 subtrapezoidal, narrowing anteriorly; axial furrow very weakly developed or absent at lateral margins of L1 (Figs. 5.3, 5.20, 9.19, 9.21, 9.24, 9.25). S2 deepest abaxially, convex anteriorly either side of axis, with adaxial and abaxial ends of each deeply incised portion on roughly transverse line. L2 subrectangular, lateral margins bowing slightly outwards. S3 pit-like. L3 subtrapezoidal, widening (tr.) anteriorly until contact with ocular lobes. LA hemispherical to transversely oblate, well inflated dorsally above extraocular area, slightly higher than posterior glabellar lobes (Fig. 5.6, 5.14, 5.23). Axial node on LO, L1, L2, and occasionally L3, decreasing in size anteriorly. Ocular lobes strongly divergent, crescentic, tip widely separated from glabella, oriented nearly straight posteriorly, posterior tip opposite midlength of L1, convex dorsally; ocular furrow not developed. Interocular area arched dorsally or sloping down from ocular lobes to axial furrow (can appear flat and shelf-like on compacted specimens), slightly wider than width (tr.) of ocular lobes and approximately half width (tr.) of extraocular area opposite L2; may bear traces of interocular nodes or swellings on cephala up to 6.7 mm sag. length (Figs. 5.1, 9.19). Posterior ocular line and intergenal ridge present on some individuals (Fig. 5.3, 5.7, 5.8, 5.9, 5.10, 5.12, 5.16–18). Genal caeca occasionally developed on extraocular area (Fig. 5.8, 5.9, 5.18). Bertillon markings on LA, passing onto ocular lobes, occasionally also onto L3 and L2. Granular ornament on central portion of LA (merging into bertillon markings laterally), posterior and lateral cephalic border (merging into bertillon markings anteriorly), interocular and extraocular areas on exceptionally well preserved specimen (Fig. 5.18–20). Terrace lines on cephalic doublure and genal spines, rarely on distal portion of posterior cephalic border (dorsal).

Mature hypostome (Fig. 6.13–22) with convex, subtriangular middle body, less convex at smaller size (Fig. 6.1–12). Anterior marginal flange narrow, weakly notched (sag.), separated from middle body by distinct furrow; anterior wing triangular, located approximately one-third distance down hypostomal length on small specimens (Fig. 6.2), approximately at hypostomal midlength on larger specimens (Fig. 6.6, 6.10, 6.14, 6.18). Posterior lobe crescentic, maximum width approximately two-thirds maximum hypostomal width, length (sag.) approximately one-quarter that of middle body, posterior margin gently curved (tr.). Furrows separating posterior lobe from middle body deep, very shallow or absent over axis, oriented strongly posteriorly

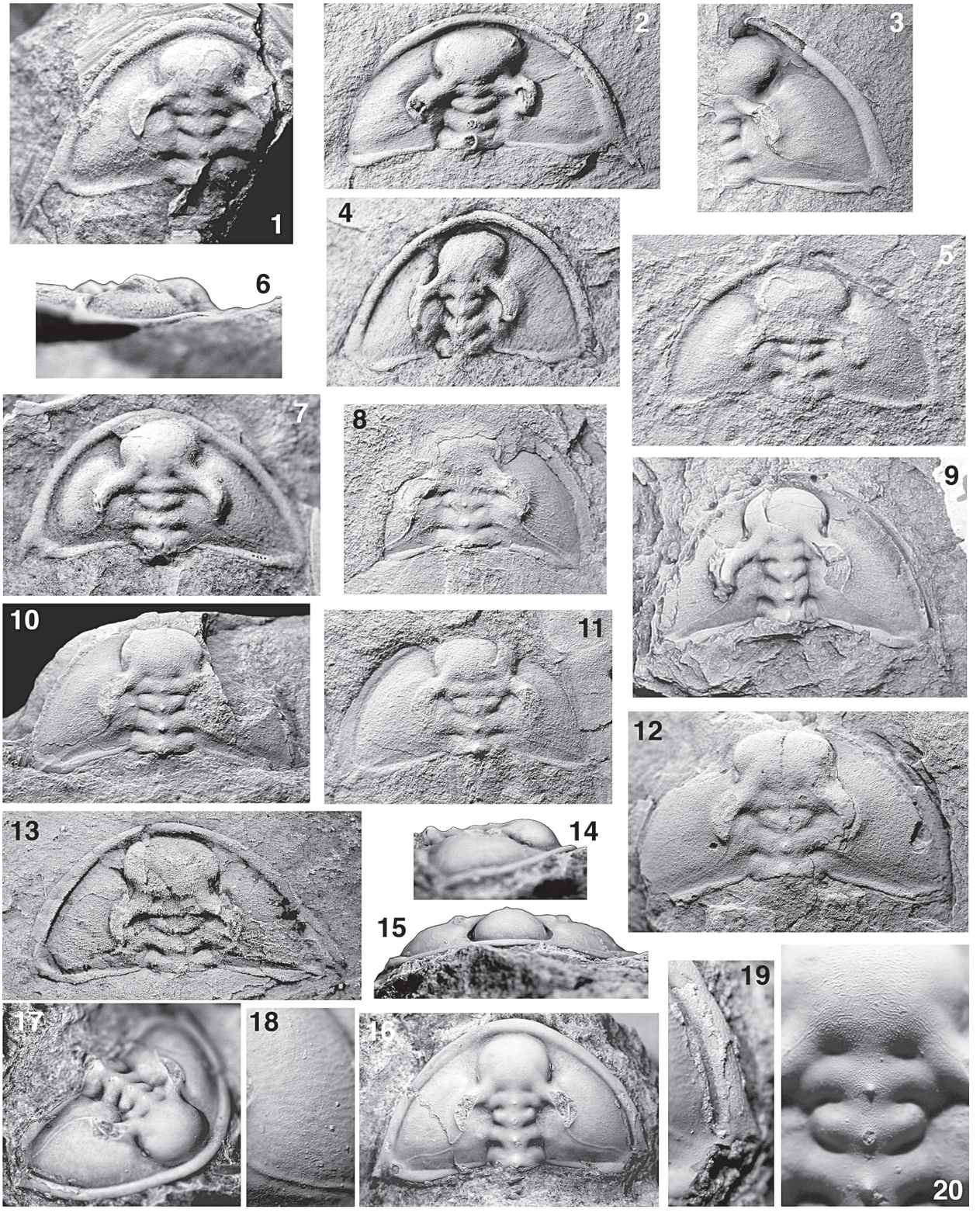

FIGURE 5—Morphological variation among cephala of *Nephrolenellus multinodus* in late phase 4 of development from various localities. See text for stratigraphic details. *1,* Incomplete but minimally compacted internal mold, dorsal view, Panamint Range, California, USNM 177228, ×4. *2, 4, 13,* Mildly tectonized cephala, latex casts of internal molds, dorsal views, Emigrant Pass section, Nopah Range, California; *2,* UCR 9989.1, ×5; *4,* UCR 9970.1, ×6; *13,* UCR 9964.1, ×4. *3,* Right half of cephalon, latex cast of external mold, dorsal view, Echo Canyon section, Funeral Mountains, California, FMNH PE57850, ×3. *5,* Poorly preserved internal mold, dorsal view, from ICS-1204, Grassy Spring section, Delamar Mountains, Nevada, FMNH PE57935, ×4. *6, 7,* Holotype cephalon, latex cast of external mold in right lateral and dorsal view, Echo Canyon section, Funeral Mountains, California, USNM 177225, ×5.

adaxially. Six pairs of marginal spines plus medial spine around margins of posterior body retained throughout ontogeny.

Prothorax (Fig. 7.1–5) of 13 segments; width (tr.) of axis approximately equal to width (tr.) of inner pleural region on T1, gently tapering posteriorly. Axial nodes developed on all segments. Inner pleural regions of T1 and T2 transverse, tapering distally, with straight margins; pleural spines sentate and divergent. T3 hyperpleural; pleural spine dolichospinous. Inner pleural region of T4 and to lesser extent T5 tapering distally. Inner pleural regions of T6 to T9 transverse, parallel-sided, with straight margins. Inner pleural regions of T10 to T13 increasingly divergent, parallel-sided, margins increasingly curved on more posterior segments. Pleural spines of T4 to T7 or T8 sentate; those of T8 or T9 to T13 increasingly falcate; all divergent, becoming subpendent on posterior segments. Pleural furrows extend onto pleural spines of T3 and T7 or T8 to T13. Pleural spine of T3 may bear granular ornament (Fig. 7.10).

Opisthothorax (Fig. 7.6–9) of at least 23 segments. Axial nodes on T14 to T17, T18, or T19, absent on more posterior segments. Inner pleural regions of T14 slightly curved, tapering, divergent; straight, parallel-sided, and divergent on all more posterior segments; pleural spines of T14 to at least T27 sentate, divergent. Pleural furrow shallow, terminating on inner pleural region, absent on segments posterior to T18 or T19. Axial furrow shallow or absent on segments posterior to T19, inner pleural region then separated from axis by break in slope only. Rest of opisthothorax and pygidium unknown.

Ontogeny.—Silicified specimens, combined with larger specimens preserved in shale, allow detailed study of the ontogeny of *Nephrolenellus multinodus* from sag. cephalic lengths of 0.49 mm to approximately 11.5 mm through all four phases of cephalic development.

Phase 1 (Fig. 8.1): Observed cephalic lengths range from 0.49 mm to 0.61 mm; two instars. Cephalon horseshoe-shaped to subcircular in outline, posterior cephalic margin straight, roughly transverse or angled very slightly posteriorly abaxially. Intergenal spines open ventrally (like an inverted gutter), posteroventrally oriented at approximately 20° from horizontal, proximal portion slightly convergent, distal portion parallel to exsag. axis; length approximately two-thirds of sag. cephalic length. Anterior border gently rounded dorsally, extends around lateral cephalic margin until contact with abaxial margin of intergenal spines; exsagittal length equal to that of LO. Border furrow shallow at sagittal axis. Preglabellar field approximately one-tenth cephalic length (sag.). Glabella slightly constricted at S3, defined by deep axial furrow, relief prominent. SO, S1, S2, and S3 transverse, deepest distally. LO ovate, exsagittal length one-tenth of sagittal cephalic length. L1, L2, and L3 subcircular, exsagittal length of each one-sixth of sagittal cephalic length. LA subcircular, inflated, summit at same dorsal elevation as more posterior glabellar lobes; sagittal length approximately one-fifth that of cephalon; not defined by axial furrow anteriorly, slopes into preglabellar field; width approximately equal to that of L1 (tr.). LO, L1, L2, L3, and LA each with prominent axial node developed centrally, node on LO smallest. Ocular lobes prominent, arcuate; strongly divergent proximally, bending to run almost parallel with exsagittal axis opposite posterior third of L3; convex dorsally; width uniform; dorsal surface inflated above level of glabella proximally, sloping posteriorly as far as opposite S1; posterior ocular line extends to abaxial margin of intergenal spines. Ocular lobes contact and run confluent with lateral cephalic border opposite L3. Interocular area shelf-like or very slightly arched dorsally. Pleural extensions of L1, L2, and L3 defined by interocular furrows; each with prominent interocular node developed midway between axial furrow and ocular lobe; summit of interocular nodes as high in relief as glabellar axial nodes. Pleural extension of L1 runs posterolaterally to base of intergenal spines as intergenal ridge.

Morphological changes between the two instars of phase 1 of cephalic development were very subtle, consisting most obviously of a slight proportional decrease in the distance between the intergenal spine bases relative to sagittal cephalic length (Fig. 2.1). A thin-plate spline deformation grid depicting patterns of cephalic shape change during this phase was presented by Webster et al. (2001, fig. 4.8a). Unfortunately, several first instar phase 1 cephala utilized in that earlier study were accidentally damaged during mounting for photography for the present paper, and further geometric morphometric analysis is not possible.

Phase 2 (Fig. 8.2–16): Observed cephalic lengths range from 0.63 mm to approximately 1.0 mm; three instars. During this phase, the proportional distance between the intergenal spine bases increased relative to sagittal cephalic length (Figs. 2.1, 10.1), the intergenal spines lengthened (to approximately same length as cephalon) and became less strongly posteroventrally oriented (Fig. 8.3, 8.6, 8.12, 8.15); and the extent of contact between the ocular lobes and the lateral cephalic border decreased until they became separated by a narrow extraocular area. Glabellar shape change was minimal and largely restricted to a subtle proportional lengthening, associated with an increase in relative size of the occipital node (Fig. 10.1). A statistical comparison of vectors of ontogenetic shape change determined that the pattern of shape change followed during phase 2 of cephalic development was significantly different from that followed during phase 1 (Webster et al., 2001; based on landmark configuration 1 as defined here [Fig. 4]).

Phase 3 (Figs. 8.17–31, 9.1–13): Observed cephalic lengths range from 1.06 mm to approximately 3.04 mm. Cephalon initially horseshoe-shaped in outline, posterior cephalic margin straight, angled slightly posteriorly abaxially. Genal spines present as small bud-like extensions of the lateral cephalic border, located immediately abaxial (and slightly ventral) to base of intergenal spines. Intergenal spines open ventrally, dipping posteroventrally at approximately 5° from horizontal, distal portion gently curved away from body axis; length approximately equal to sag. cephalic length. Cephalic border well defined around entire cephalon by distinct border furrow; gently rounded dorsally anteriorly; width of anterior border opposite junction of ocular lobes with LA approximately equal to length (exsag.) of LO. Preglabellar field slightly shorter than width of anterior cephalic border (sag.). Glabella constricted at S3, defined by deep axial furrow. SO, S1, S2, and S3 transverse, deepest distally. LO transversely ovate, length (exsag.) approximately one-tenth of sag. cephalic length; approximately as wide as L1. L1, L2, and L3 subrectangular to trapezoidal, successively narrowing slightly anteriorly; each approximately one-seventh sag. cephalic length. LA subcircular, slightly inflated, summit at same dorsal elevation as more posterior glabellar lobes; sagittal length approximately one-quarter that of cephalon; not prominently separated from preglabellar field anteriorly; maximum width slightly wider than that of LO (tr.). LO, L1, L2, L3, and LA each with prominent axial node developed centrally, node on LA smallest. Ocular lobes prominent, convex dorsally, dorsal surface above level of glabella (Fig. 8.20), crescentic; strongly divergent proximally, bending to run almost parallel with exsagittal axis opposite midlength of L3, posterior tips slightly convergent; posterior tip opposite L1. Interocular area shelf-like or very slightly arched dorsally. Pleural extensions of L1, L2, and L3 defined by interocular furrows; each with prominent interocular node developed midway between axial furrow and ocular

←

8–12, Internal molds of varying preservational quality, dorsal views, showing traces of extraocular caeca, posterior ocular lines, and intergenal ridges, Frenchman Mountain, Nevada; *8,* UCR 9961.7, ×5; *9,* UCR 9961.20, ×4; *10,* UCR 9961.3, ×4; *11,* UCR 9961.16, ×4; *12,* UCR 9961.13, ×4. *14–20,* Cephalon preserved in limestone showing fine details of exoskeletal ornament, Jasper Park, Alberta, GSC 16858; *14,* right lateral view, ×3; *15,* anterior view, ×3; *16,* dorsal view, ×3; *17,* oblique right anterolateral view, ×3; *18,* details of ornament on right extraocular area, ×8; *19,* details of ornament on right lateral border (partially exfoliated), ×8; *20,* details of ornament on glabella, ×8.

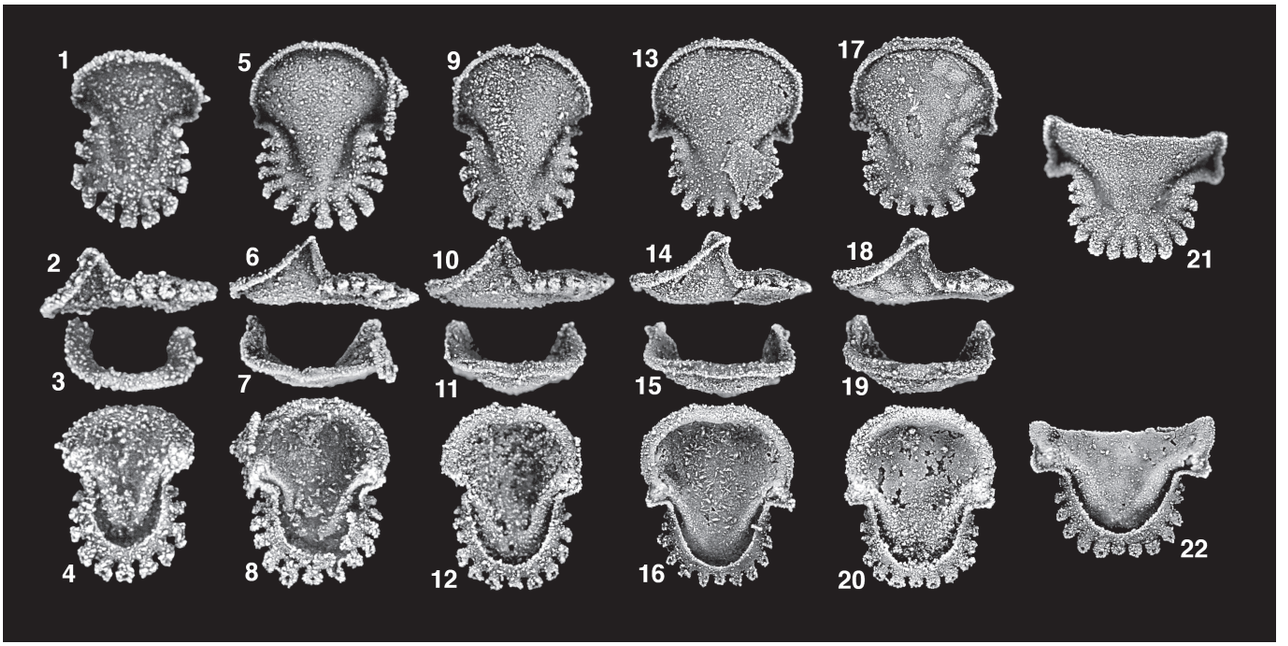

FIGURE 6—Ontogenetic development of the hypostome of *Nephrolenellus multinodus*, larger specimens to the right. *1–4,* Small hypostome in ventral, left lateral, anterior, and dorsal views, FMNH PE57851, ×20. *5–8,* FMNH PE57852 in ventral, right lateral, anterior, and dorsal views, ×15. The right lateral view has been computationally reflected for consistency with views of other specimens. *9–12,* FMNH PE5784 in ventral, left lateral, anterior, and dorsal views, ×13. *13–16,* FMNH PE5785 in ventral, left lateral, anterior, and dorsal views, ×10. *17–20,* FMNH PE5786 in ventral, left lateral, anterior, and dorsal views, ×10. *21, 22,* Large but incomplete hypostome in ventral and dorsal views, FMNH PE5787, ×10. All from ICS-1158, Oak Spring Summit section, Delamar Mountains, Nevada. See text for stratigraphic details.

lobe; summit of interocular nodes slightly subdued below relief of glabellar axial nodes. Pleural extension of L1 runs posterolaterally to base of intergenal spines as intergenal ridge. Posterior ocular line sweeps from posterior tip of ocular lobe to merge with abaxial margin of intergenal spine.

Considerable morphological change occurred during phase 3 of cephalic development (see also Fig. 10.2). The extraocular area continued to widen, the posterior cephalic margin elongated, and a weak adgenal angle developed at about the midlength of posterior margin (Fig. 9.13). An anterior arch is present on cephala in late phase 3 of development (contrast Figs. 8. 20, 8.25, 8.28. 8.33, 9.4, 9.12). The genal spines elongated, such that they are stubby, blunt, structures approximately equal in length to LO (exsag.) immediately adjacent to the intergenal spines on cephala in late phase 3 of development (Fig. 9.9, 9.13). The intergenal spines became more posterolaterally directed and proportionally shortened, being less than one quarter of sagittal cephalic length on late phase 3 cephala (Fig. 9.9). LO proportionally widened and lengthened, such that the glabella tapers evenly anteriorly to L2 or S3 on late phase 3 cephala. LA continued to proportionally increase in length and width, and L3 proportionally shortened (exsag.) and widened (tr.), increasing its extent of contact with the adaxial margin of the ocular lobes. On cephala in late phase 3 of development LA is dorsally inflated above the level of more posterior glabellar lobes, is slightly wider (tr.) than LO, and is separated from the preglabellar field by a distinct axial furrow (Fig. 9.9, 9.11–13). The preglabellar field is less than half the length (sag.) of the anterior cephalic border. The axial node on LA is absent on large phase 3 cephala, the node on L3 reduced in size, the node on LO more spine-like, and the interocular nodes are rather subdued or absent, although the interocular furrows remain as very shallow depressions (Fig. 9.5, 9.13). The ocular lobes are of mature morphology, and the posterior ocular line and intergenal ridge are much reduced in prominence (the latter may be absent) relative to ontogenetically younger cephala. Terrace lines on the cephalic doublure and ventral surface of the genal spines first become visible on cephala in phase 3 of development (Figs. 8.23, 8.24, 8.27, 9.2–4, 9.6, 9.7, 9.10–12).

The pattern of cephalic shape change followed during phase 3 of development (Fig. 10.2) appears to be markedly different to that followed during phase 2 of development (Fig. 10.1). Using landmark configuration 2, statistical comparison of vectors of ontogenetic shape change determined that the pattern of shape change followed during phase 3 of cephalic development ($n = 20$) was significantly different from that followed during phase 2 ($n = 12$; between-phase angle of 90.9° based on vectors derived from Bookstein coordinates or 78.9° based on vectors derived from warp scores [reference form = consensus form of first instar in phase 2 of development], both significant at 95% confidence based on bootstrap resampling [400 iterations]). An earlier study (Webster et al., 2001) failed to find significant a difference in pattern of shape change between phases 2 and 3, but was based on a smaller sample size.

Phase 4 (Figs. 9.14–26, 5, 7): Observed cephalic lengths range from 3.15 mm to approximately 11.5 mm. Cephalon initially roughly semicircular in outline, proximal portion of posterior cephalic margin angled slightly posteriorly abaxially, distal portion deflected into less strong posterolateral orientation at adgenal angle located midway along posterior cephalic margin. Genal spines slender, approximately one-eighth of sagittal cephalic length, base opposite point behind posterior margin of LO, immediately lateral to base of intergenal spines. Intergenal spines almost closed ventrally into cylindrical cross-section (Fig. 9.15), posterolaterally oriented; length approximately one-tenth that of cephalon (sag.). Cephalic border well defined around entire cephalon by distinct border furrow; rounded dorsally anteriorly; width of anterior border opposite junction of ocular lobes with LA approximately three-quarters length (exsag.) of LO; posterior border narrows adaxially. Preglabellar field very short, length (sag.) slightly less than half that of anterior cephalic border and about one-quarter

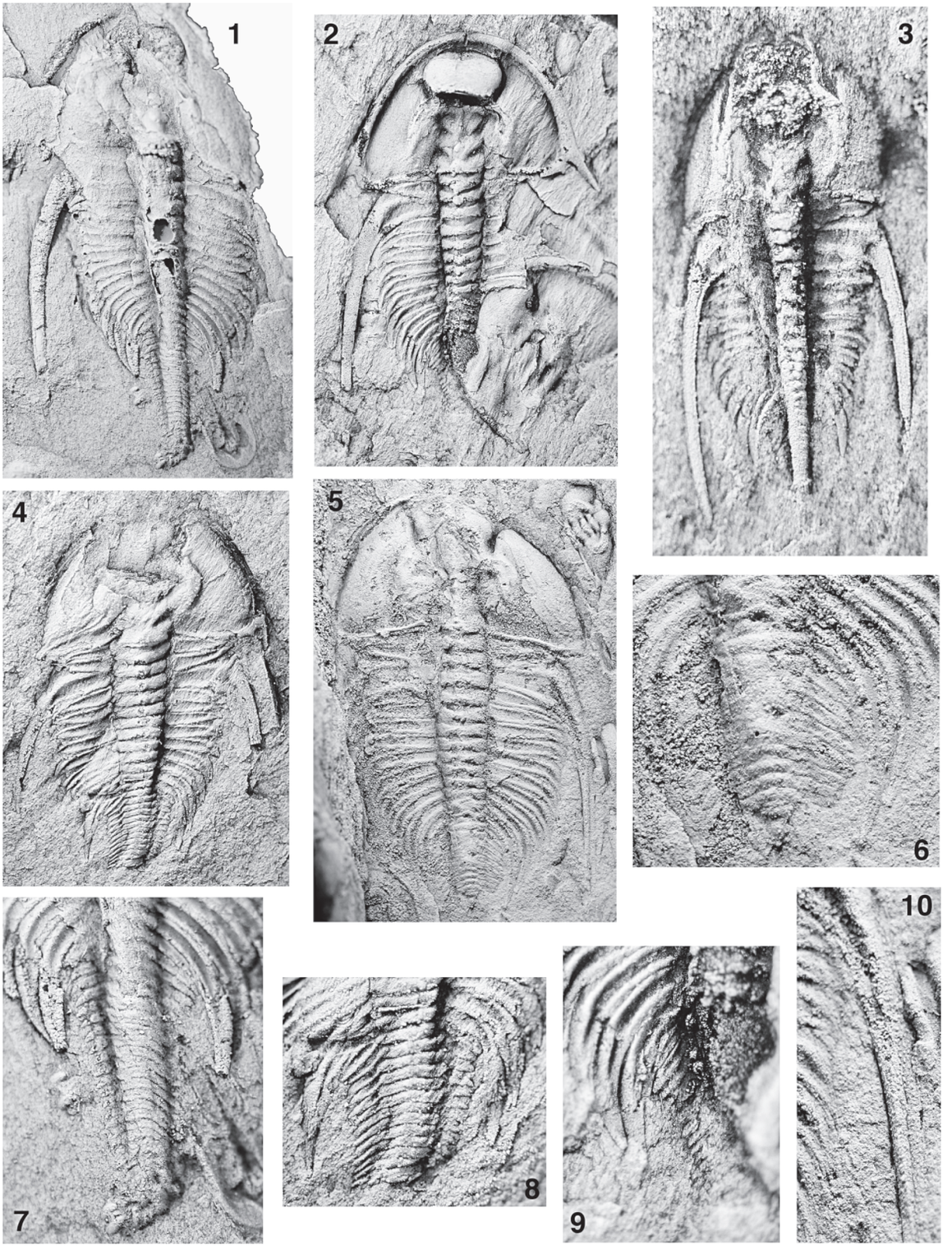

FIGURE 7—Articulated specimens of *Nephrolenellus multinodus* in phase 4 of cephalic development showing details of the prothorax and opisthothorax. *1, 7*, UCR 9968.1. *1*, Almost complete dorsal exoskeleton, ×5; *7*, details of opisthothorax, ×10. *2, 9*, UCR 9966.1. *2*, Almost complete dorsal exoskeleton, ×4; *9*, details of opisthothorax, ×10. *3*, Almost complete dorsal exoskeleton, UCR 9967.2, ×8. *4, 8,* UCR 9969.1. *4*, Almost complete dorsal exoskeleton, ×5; *8*, details of opisthothorax, ×10. *5, 6, 10,* UCR 9965.2. *5*, Almost complete dorsal exoskeleton, ×4; *6*, details of opisthothorax, ×10; *10*, enlargement of pleural spine of third thoracic segment showing granular ornament, ×10. All are dorsal views of latex casts of mildly tectonized external molds from Emigrant Pass section, Nopah Range, California. See text for stratigraphic details.

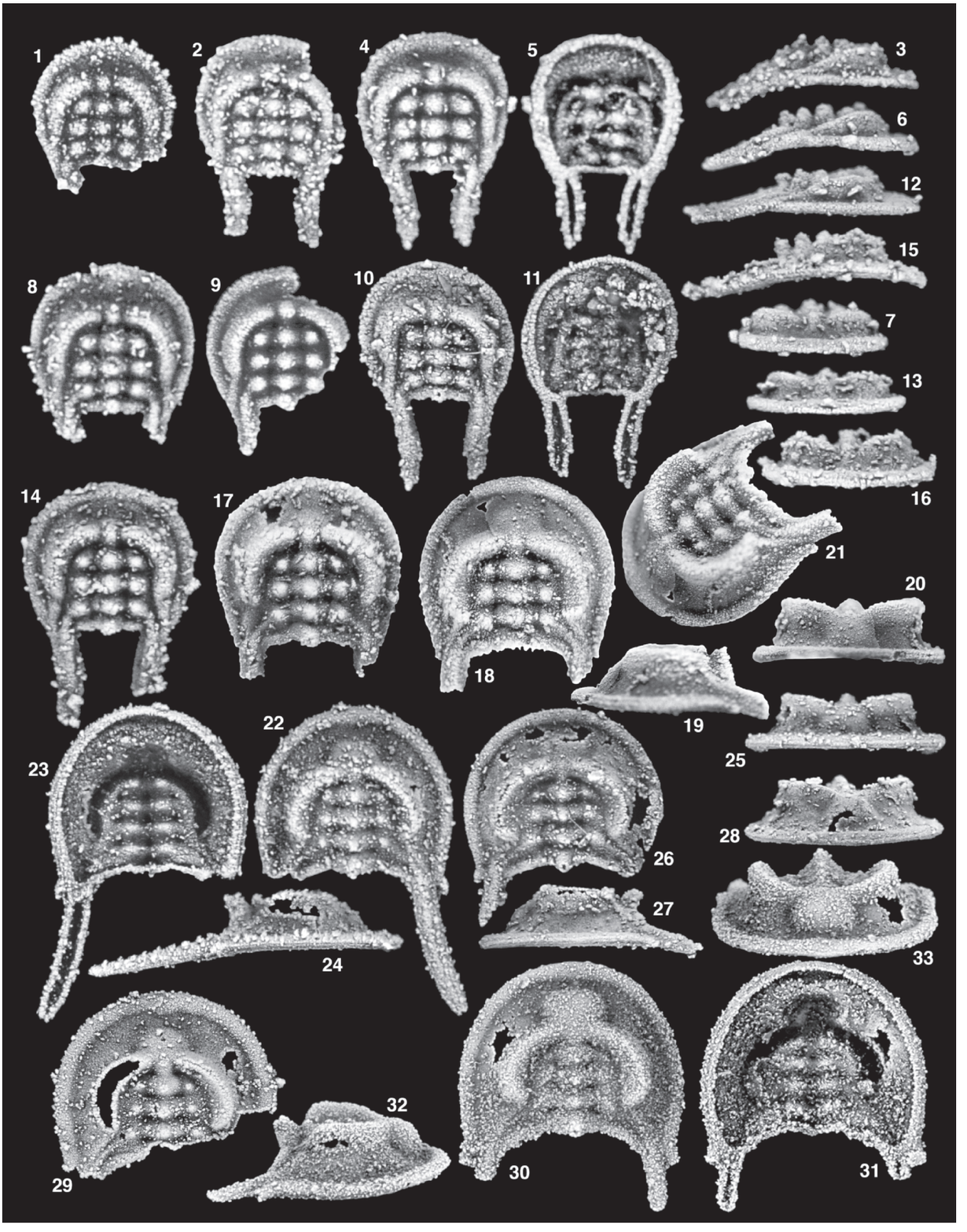

FIGURE *8*—Silicified specimens representing the ontogenetic development of the cephalon of *Nephrolenellus multinodus* (phases 1 through 3). *1*, Cephalon in phase 1 of development (instar two), dorsal view, FMNH PE57860, ×40. Intergenal spines missing. *2, 3*, Slightly broken cephalon in phase 2 of development (instar three), dorsal and left lateral views, FMNH PE57887, ×40. The left lateral view has been computationally reflected for consistency with views of other specimens. *4–7*, Cephalon in phase 2 of development (instar three), dorsal, ventral, right lateral, and anterior views, FMNH PE57888, ×40. *8*, Cephalon in phase 2 of development (instar four), dorsal view, FMNH 57884, ×37. Tips of intergenal spines missing. *9,* Incomplete cephalon in phase 2 of development (instar four), dorsal view, UCR 9949.21, ×37. *10–13*, Cephalon in phase 2 of development (instar five), dorsal, ventral, right lateral, and anterior views,

that of LO (exsag.). Glabella constricted at L2. Maximum width of LA approximately one-third wider (tr.) than basal glabellar width. Posterior margin of glabella gently convex posteriorly. SO deep only abaxially, well incised portions each gently convex anteriorly. S1 and S2 deepest abaxially, oriented slightly anterolaterally abaxially (S1 more strongly so). LO and L1 subtrapezoidal, narrowing anteriorly; axial furrow shallow at lateral margins of L1. L2 subrectangular, lateral margins bowing slightly outwards. S3 absent over axis, shallow along contact between L3 and ocular lobes, deepest in pit-like position midway between axial furrow and sagittal axis. L3 subtrapezoidal, widening (tr.) anteriorly until contact with ocular lobes. LA hemispherical to transversely oblate, well inflated dorsally above extraocular area, slightly higher than posterior glabellar lobes (Fig. 9.16, 9.17). Axial spine on LO, axial node on L1, L2, and L3, decreasing in size anteriorly. Ocular lobes strongly divergent, crescentic, tip widely separated from glabella, oriented nearly straight posteriorly, posterior tip opposite posterior third of L1, convex dorsally; ocular furrow not developed. Interocular area shelf-like, slightly wider than width (tr.) of ocular lobes and approximately equal to width (tr.) of extraocular area opposite L2; interocular furrows absent. Posterior ocular line and intergenal ridge weak or absent. A specimen with sag. cephalic length 2.7 mm possesses all 13 prothoracic segments (opisthothorax, if present, and pygidium not preserved).

Phase 4 morphology of cephala >5 mm length (sag.) was described above. Morphological changes during early phase 4 include relative elongation of the posterior cephalic border between the axial furrow and the intergenal spines, and between the intergenal and genal spines. LA continued to proportionally enlarge in all dimensions, and L3 continued to proportionally laterally widen. L2 underwent a marked relative shortening (exsag.), and L1 became proportionally slightly longer (exsag.). The interocular area first becomes arched or sloping on cephala approximately 3.5 mm long (sag.). Ornament such as genal caeca on the extraocular area and bertillon markings on LA first become apparent on cephala 4.2 mm long (sag.). By cephalic length of approximately 4.1 mm (sag.) at least 15 opisthothoracic segments had been released (Fig. 7.3), and at least 23 opisthothoracic segments are present on an otherwise poorly preserved specimen with sag. cephalic length of approximately 4.8 mm (pygidium not preserved in either case).

Cephala of *N. multinodus* in phase 4 of development are rarely preserved intact in a silicified state. To bolster sample size in quantitative analyses of patterns of shape change over this portion of ontogeny it is possible to incorporate data from specimens preserved in shale, although the morphology of these specimens has been taphonomically altered. Using landmark configuration 3 and combining data from silicified and non-silicified specimens, Webster et al. (2001) found a statistically significant (to 95% confidence) difference in pattern of shape change between phases 3 and 4 of cephalic development (based on vectors derived from Bookstein registration and sliding baseline registration coordinates, but not from warp scores). However, a significant change in allometric patterning across this transition was not detected in the present analysis using landmark configuration 3 (phase 3, n = 6; phase 4, n = 8; between-phase angle of 38.7° based on vectors derived from Bookstein coordinates or 32.4° based on vectors derived from warp scores [reference form = smallest cephalon in phase 3 of development], neither significant at 95% confidence based on bootstrap resampling [400 iterations]) or landmark configuration 4 (phase 3, n = 13; phase 4, n = 19; between-phase angle of 35.1° based on vectors derived from Bookstein coordinates or 36.0° based on vectors derived from warp scores [reference form = consensus form of second instar in phase 1 of development], neither significant at 95% confidence based on bootstrap resampling [400 iterations]) despite a larger sample size. This failure to recover a significant difference between phases 3 and 4 is surprising, given the apparent change in allometry of glabellar lobes L1 and L2 in particular (compare Fig. 10.2 and 10.3) and the results of the previous study, but likely results from a combination of taphonomic overprint on phase 4 cephala and the conservative nature of the bootstrap resampling procedure. In all analyses, failure to reject the null hypothesis resulted from high variance within phase 4 of development (based on bootstrap resampling).

Holotype.—USNM 177225, designated by Palmer in Palmer and Halley (1979, pl. 4, fig. 4; Fig. 5.6, 5.7 herein).

Occurrence.—CALIFORNIA: *Marble Mountains, San Bernardino County:* UCR 9976, shales 16.93 m to 17.00 m above top of Chambless Limestone cliff, Cadiz Formation. Palmer and Halley (1979, p. 73) document this species from a "2.5-cm limestone bed immediately above the Chambless Limestone" from this section, although they likely considered the basal 16.61 m of the Cadiz Formation (the limestone-rich "transitional facies") to be part of the Chambless Limestone. *Resting Springs Range, Inyo County:* USGS locality 3676-CO, Pyramid Shale Member, Carrara Formation (Palmer and Halley, 1979). *Nopah Range, Inyo County:* Emigrant Pass section, throughout basal 22 m of Pyramid Shale Member, Carrara Formation (Fowler, 1999), including UCR 9964, UCR 9965, UCR 9966, UCR 9967, UCR 9968, UCR 9969, UCR 9970, UCR 9971, UCR 9972, and UCR 9989. *Eagle Mountain, Inyo County:* 9 m, 10.6 m, 11.7 m, 12 m, and 15.8 m above base of Pyramid Shale Member (Ed Fowler collection, including UCR 9973 and UCR 9974), and ICS-1297 (18.5 m above base of Pyramid Shale Member), Carrara Formation. Also USGS locality 3681-CO (Palmer and Halley, 1979). *Grapevine Mountains, Inyo County:* Titanothere Canyon section, 8.5 m, 10 m, and 11 m above base of Pyramid Shale Member, Carrara Formation (new collections), also USGS localities 3698-CO and 7184b-CO (Palmer and Halley, 1979) from lower in the same member. *Funeral Mountains, Inyo County:* Echo Canyon section, basal 2 m, 3 m, about 4 m, 4-5 m, and 5 m above base of Pyramid Shale Member, Carrara Formation (new collections), also USGS localities 2304-CO and 3097-CO (Palmer and Halley, 1979). Pyramid Peak section, float from basal Pyramid Shale Member, Carrara Formation (new collections), also Palmer and Halley (1979). *Panamint Range, Inyo County:* USGS locality 3095-CO (Palmer and Halley, 1979). NEVADA: *? Virgin Mountains, Clark County:* UCR 10230, sandstone in Bright Angel Shale, collected from ridge south of Whitney Ranch (collected by Mason and Hazzard in 1936, see Longwell, 1928, p. 23 for section details). *Frenchman Mountain, Clark County:* UCR 9961, Bright Angel Shale. *Desert Range, Clark County:* USGS locality 3696a-CO, Pyramid Shale Member, Carrara Formation (Palmer and Halley, 1979). *Burnt Springs Range, Lincoln County:* Hidden Valley section, ICS-1279, carbonate nodules approximately 1 m above uppermost limestone ledge of cliffy portion of Combined Metals Member, Pioche Formation (Fig. 1; see Palmer [1998] for locality details). *Delamar Mountains, Lincoln County:* Oak Spring Summit section, ICS-1158, carbonate nodules 0.25 m below uppermost limestone ledge of cliffy portion of Combined Metals Member (4.7 m above basal ledge of Combined Metals Member, 7.4 m below ribbon carbonate marking base of Middle Cambrian), Pioche Formation (Palmer, 1998); ICS-1033, carbonate nodules 5.5 m above uppermost limestone ledge of cliffy portion of Combined Metals Member, Pioche Formation. Seven Oaks Spring section, ICS-1114, uppermost limestone nodules of cliffy portion of Combined Metals Member, Pioche Formation (see Palmer [1998] for locality details). Grassy

←

FMNH PE57889, ×32. *14–16*, Cephalon in phase 2 of development (instar five), dorsal, right lateral, and anterior views, FMNH PE57890, ×32. Tip of right intergenal spine missing. *17*, Cephalon in phase 3 of development, dorsal view, UCR 9949.5, ×30. Tips of intergenal spines missing. *18–21*, Cephalon in phase 3 of development, dorsal, left lateral, anterior, and oblique left anterolateral view, UCR 9949.6, ×22. Tips of intergenal spines missing. *22–25*, Cephalon in phase 3 of development, dorsal, ventral, right lateral, and anterior views, FMNH PE57930, ×20. Left intergenal and genal spines missing. *26–28*, Cephalon in phase 3 of development, dorsal, left lateral, and anterior views, FMNH PE57892, ×18. Right intergenal and genal spines plus tip of left intergenal spine missing. *29,* Incomplete cephalon in phase 3 of development, dorsal view, FMNH PE57917, ×18. *30–33*, Coarsely silicified cephalon in phase 3 of development, dorsal, ventral, right lateral, and anterior views, FMNH PE57923, ×15. Tips of intergenal spines missing. Specimens in figures 1–8, 10–16, and 26–28 from ICS-1158, Oak Spring Summit section, Delamar Mountains, Nevada. Specimens in figures 9 and 17–21 from Groom Range, Nevada. Specimens in figures 22–25 and 29–33 from ICS-1279, Hidden Valley section, Burnt Springs Range, Nevada. See text for stratigraphic details.

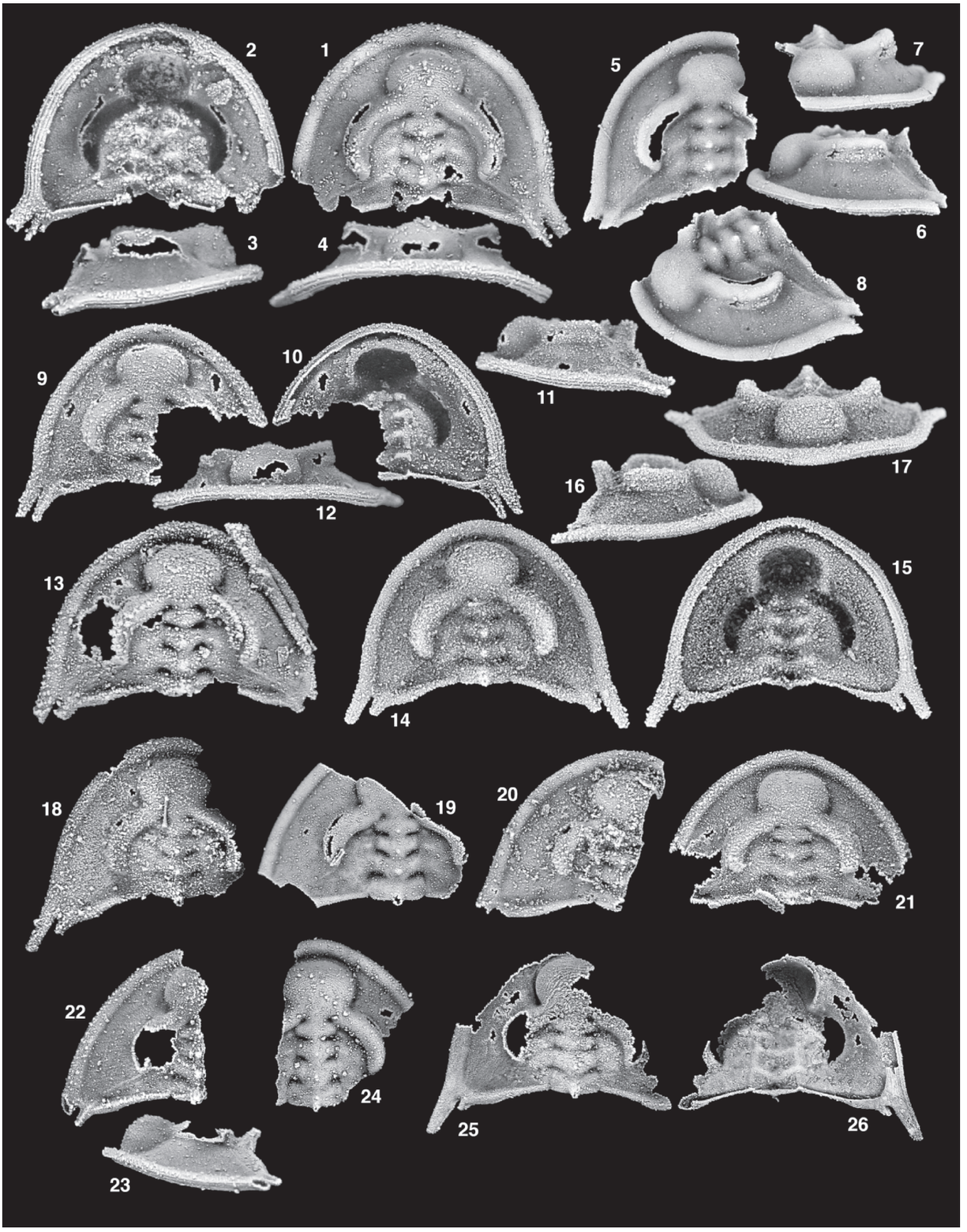

FIGURE 9—Silicified specimens representing the ontogenetic development of the cephalon of *Nephrolenellus multinodus* (phases 3 and 4). *1–4*, Slightly broken cephalon in phase 3 of development, dorsal, ventral, right lateral, and anterior views, FMNH PE57898, ×13. *5–8,* Incomplete cephalon in phase 3 of development, dorsal, left lateral, anterior, and oblique left anterolateral views, UCR 9949.9, ×12. *9–12*, Incomplete cephalon in phase 3 of development, dorsal, ventral, left lateral, and anterior views, FMNH PE57894, ×10. *13*, Slightly broken cephalon in phase 3 of development, dorsal view, FMNH PE57900, ×10. *14–17,* Cephalon in phase 4 of development, dorsal, ventral, right lateral, and anterior views, FMNH PE57925, ×10. *18,* Incomplete cephalon in phase 4 of development, dorsal view, FMNH PE57941, ×9. *19*, Incomplete cephalon in phase 4 of development, dorsal view, FMNH PE57927, ×8. *20*, Incomplete

Spring section, ICS-1204, ICS-1205, and ICS-1283 (shales 5 m and 6 m above uppermost limestone ledge in cliffy portion of Combined Metals Member, 10 m below ribbon carbonate marking base of Middle Cambrian), Pioche Formation (see Palmer [1998] for locality details). *Chief Range, Lincoln County:* Ruin Wash section, ICS-1049, carbonate nodules approximately 5-6 m below ribbon carbonate marking base of Middle Cambrian (see Palmer [1998] for locality details). *? Highland Range, Lincoln County:* questionable occurrence immediately below the ribbon carbonate marking the base of the Middle Cambrian (Sundberg and McCollum, 2000). *Groom Range, Lincoln County:* UCR 9949, carbonate ledge 27.13 m to 27.17 m above top of highest continuous limestone ledge of ''Gold Ace Limestone''; also shales 18.1 m to 27.8 m above top of highest continuous limestone ledge of ''Gold Ace Limestone'' (new collections). CANADA: *Jasper Park, Alberta:* GSC locality 42591, from a thin, argillaceous, gray wackestone 10 m above the top of the Gog Group, about 2 miles (3.3 km) southwest of Mount Simla (Norford, 1962; Mountjoy, 1962).

Discussion.—Based on examination of a much larger sample size (Appendix, accessed in Supplemental Data Archive at www.journalofpaleontology.org), the original description of the mature morphology of *Nephrolenellus multinodus* is expanded (above), and thoracic morphology and the ontogenetic development of the cephalon is detailed for the first time. Previous references to the thorax of this species (Stitt and Clark, 1984; Whittington, 1989; Lieberman, 1998) relate to a specimen since referred to *N. geniculatus*.

A single specimen (GSC 16858) figured by Norford (1962, pl. 1, fig. 3; also Palmer and Halley, 1979, pl. 4, fig. 6; Lieberman, 1999, fig. 20.6; Fig. 5.14–20 herein) collected from Alberta was assigned to *Nephrolenellus multinodus* by Palmer in Palmer and Halley (1979, p. 73). Lieberman (1998, 1999), however, designated the specimen as the holotype (and only known specimen) of a new species, *N. jasperensis* Lieberman, 1999. Lieberman's (1999) description of the Canadian specimen is erroneous in several respects: the presence of an ocular furrow cannot be determined (the ocular lobes are incompletely preserved; Fig. 5.16), a small intergenal spine can be seen (although it is chipped at the base; Fig. 5.16), and weak extraocular genal caeca are visible (Fig. 5.18). The frontal lobe of the glabella is separated from the anterior border by a wide furrow (Fig. 5.16, 5.17) as is observed in large *N. multinodus* from the Great Basin (Fig. 5.2, 5.13). Other aspects of the ornament on the Canadian specimen (granulations on LA, grading into bertillon markings on the adaxial portion of the ocular lobes [Fig. 5.20]; very weak intergenal ridge; posterior ocular line [Fig. 5.16, 5.18) were not mentioned by Lieberman (1999), but are seen on some specimens of *N. multinodus* from the Great Basin (e.g., Figs. 5.9, 5.10, 9.24, 9.25). Lieberman (1998, 1999) based his distinction between *N. jasperensis* and *N. multinodus* on: 1) the location of the adgenal angle along the posterior cephalic margin (character 3 in Lieberman's [1999, p. 133] cladistic analysis of *Bolbolenellus* Palmer and Repina, 1993; coded as ''directly behind genal spine'' in *N. multinodus*, and as ''two-thirds of the way between distal tip of ocular lobes and genal spine base'' in *N. jasperensis*); 2) the nature of glabella furrows (S3 and SO each conjoined medially in *N. jasperensis*, not so in *N. multinodus*); and 3) higher vaulting of the extraocular area in *N. jasperensis*. In fact, *N. multinodus* from the Great Basin exhibits considerable variability in both the location of the adgenal angle (including the condition seen in *N. jasperensis*; Fig. 5.2, 5.4, 5.9), and in the depth of incision of S3 and SO over the glabella axis (a feature highly prone to taphonomic alteration in any case) (e.g., Fig. 5.2, 5.11). Well preserved specimens of *N. multinodus* (preserved in a silicified or minimally compacted state; Figs. 9.23, 5.6) reveal that the vaulting of the extraocular area is not noticably different to that seen in the noncompacted Canadian specimen (preserved in a limestone; Fig. 5.14).

Rigorous quantitative comparison of cephalic shape is hindered by the nature of preservation of the genal region of the Canadian specimen (the better preserved left genal region has been fractured, displaced and slightly rotated relative to the rest of the cephalon; Fig. 5.16). Nevertheless, visual comparison reveals the cephalic shape (including location of the adgenal angle and intergenal spine) of the Canadian specimen falls well within the bounds of morphological variation expressed by the Great Basin material (Fig. 5). This is corroborated by morphometric analysis of glabellar shape (e.g., Fig. 11). No feature consistently discriminates between the Canadian specimen and the Great Basin material. As a result, *N. jasperensis* is here considered a junior synonym of *N. multinodus*.

The present study brings to light several unrecognized polymorphisms and mis-codings of character states for *N. multinodus* in a recent cladistic analysis of olenelloid trilobite phylogeny (Lieberman, 1998). The preglabellar field (character 5) is progressively reduced during ontogeny, but is still present on all but the largest cephala (up to 8 mm sagittal length; state 0). Character 5 is therefore ontogenetically polymorphic (states 0 and 1; coded as state 1 in the original) unless coding is restricted to only the largest specimens. The length of LA (character 9) is typically between 1.25 and 1.5 times the sagittal length of LO and L1 (Fig. 5) and is occasionally longer. The typical values therefore fall between states 0 (equal to the length of LO and L1) and 1 (equal to 1.5 times the length of LO and L1 medially) as defined by Lieberman (1998), but are closer to state 1 (coded as state 0 in the original). The surface of the interocular area slopes from the ocular lobe to the glabella or is arched (states 0 and 2; coded as state 1 [flattened shelf] in the original). The course of S3 (character 27) is difficult to determine owing to its pit-like incision. The proximal end of the distal portion of SO (character 37) is slightly posterior to its distal end (state 0; coded as state 1 [transverse] in the original). Polymorphism in the degree of convexity of the posterior margin of LO and the development of extraocular genal caeca and an intergenal ridge (characters 41, 45, and 48; all states 0 and 1) was not recognized in the original. The location of the base of the genal spine is variably developed opposite or posterior to LO, and character 52 is therefore polymorphic (states 0 and 4; coded only as state 0 [opposite LO] in the original). None of the 14 specimens on which the angularity of the ''intergenal angle'' (the adgenal angle as defined in the present paper) could be reliably made showed a value of more than 50°, and character 55 should be coded as state 1 (directed anteriorly at roughly 45°) rather than state 2 (directed anteriorly at 60° to 70°). The thoracic characters (57 to 77) were coded by Lieberman (1998) from a specimen now recognized as *N. geniculatus*. Correct character states for *N. multinodus* should be: 011210(1,2)010(0,1)000?100001. Polymorphisms in characters 63 and 67 relate to changes in length of thoracic pleural spines and thoracic pleural furrows down the length of the thorax; these polymorphisms could be removed if the characters related to more specific segments.

Differences between *Nephrolenellus multinodus* and *N. geniculatus* are discussed below.

←

cephalon in phase 4 of development, dorsal view, FMNH PE57932, ×8 *21*, Incomplete cephalon in phase 4 of development, dorsal view, FMNH PE57895, ×8. *22, 23*, Incomplete cephalon in phase 4 of development, dorsal and left lateral views, FMNH PE57899, ×8. *24*, Incomplete cephalon in phase 4 of development, dorsal view, FMNH PE57897, ×8. *25, 26,* Incomplete cephalon in phase 4 of development, dorsal and ventral views, FMNH PE57902, ×7. Specimens in figures 1–4, 9–13, and 21–26 from ICS-1158, Oak Spring Summit section, Delamar Mountains, Nevada. Specimens in figures 14–17, 19, 20, from ICS-1279, Hidden Valley section, Burnt Springs Range, Nevada. Specimen in figure 18 from ICS-1049, Ruin Wash section, Chief Range, Nevada. Specimens in figures 5–8 from Groom Range, Nevada. See text for stratigraphic details.

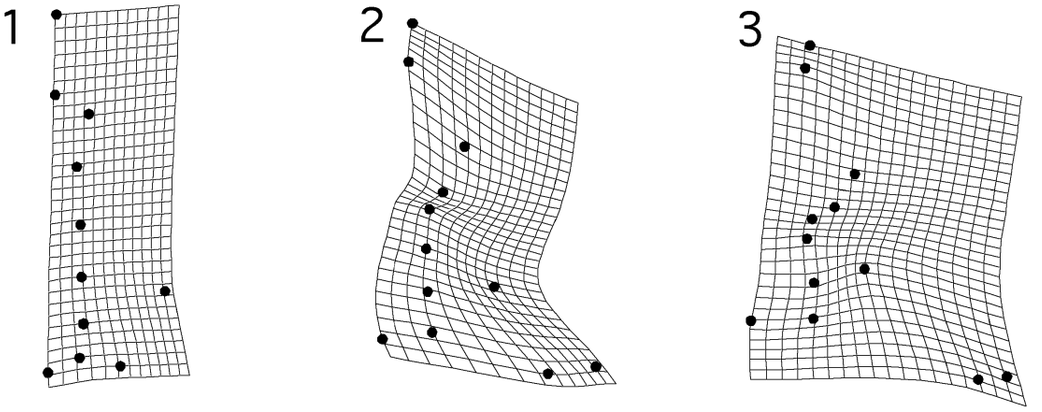

FIGURE *10*—Thin-plate spline deformation grids depicting patterns of shape change during successive phases of cephalic development in *Nephrolenellus multinodus*. *1,* Phase 2 of cephalic development, landmark configuration 1. *2*, Phase 3 of cephalic development, landmark configuration 3. *3*, Phase 4 of cephalic development, landmark configuration 3. See Fig. 4 for details of landmark configurations.

NEPHROLENELLUS GENICULATUS Palmer, 1998
Figures 12, 13, 14, 15, 16, 17

Nephrolenellus geniculatus PALMER, 1998, pp. 653, 656, 657, 659–661, figs. 5.4, 6.1–9, 6.11–13; WEBSTER AND HUGHES, 1999, pp. 358–365, 368, 369, figs. 1.3–4, 2.3–4; PALMER, 1999a, fig. 20.4; PALMER, 1999b, p. 27; FOWLER, 1999, pp. 47, 49, 50; SUNDBERG, 2000, p. 266, fig. 7b; SUNDBERG AND MCCOLLUM, 2000, p. 606 [listed in biostratigraphic range chart]; WEBSTER, SHEETS, AND HUGHES, 2001, pp. 106, 110–136, figs. 4.2e–h; HUGHES, 2003, p. 193; WEBSTER, SADLER, KOOSER, AND FOWLER, 2003, figs. 2, 9, 10 [listed in biostratigraphic range charts]; WEBSTER AND ZELDITCH, 2005, pp. 366–370, figs. 3–6; PATERSON AND EDGECOMBE, 2006, pp. 498, 499

Olenellus sp. undet. ? RESSER *in* MCKEE, 1945 (part), p. 193, pl. 19, fig. 23 only

Olenellus multinodus PALMER *in* PALMER AND HALLEY, 1979 (part), pl. 4, figs. 7, 8 only; STITT AND CLARK, 1984, p. 149 [referring to Palmer and Halley, 1979, pl. 4, figs. 7, 8]; WHITTINGTON, 1989, pp. 131, 132, 133 [referring to Palmer and Halley, 1979, pl. 4, fig. 7]

Nephrolenellus multinodus ? SUNDBERG AND MCCOLLUM, 1997 (part), p. 1068 [listed in biostratigraphic chart—refers at least in part to *Nephrolenellus geniculatus*]; LIEBERMAN, 1998 (part), p. 62 [includes some details of *N. geniculatus*]

Nephrolenellus sp. PALMER AND REPINA, 1993, fig. 4.3; PALMER AND REPINA, 1997, p. 409, fig. 258.4b

Description (mature morphology).—Cephalon semicircular in outline; proximal portion of posterior cephalic margin angled slightly posteriorly away from axial furrow, distal portion flexing anteriorly by 35° to 60° relative to proximal portion at distinct adgenal angle located approximately two-thirds distance from axial furrow to base of genal spine. Greatest observed cephalic length approximately 11.8 mm (sag.). Genal spine slender, base opposite midlength of LO; length just less than half cephalic length (sag.). Intergenal nubbin or node between adgenal angle and base of genal spine (closer to genal spine), weak or absent on cephala >6 mm long (sag.) (Fig. 17.13). Cephalic border well defined around entire cephalon by distinct border furrow; rounded dorsally anteriorly, flattening slightly towards base of genal spine; width of anterior border opposite junction of ocular lobes with LA three-fifths length (exsag.) of LO; posterior border narrows adaxially. Glabella hourglass-shaped, constricted at L2; touches and slightly deflects anterior border furrow (Figs. 12.3, 12.4, 14.6, 17.5, 17.8, 17.13). Maximum width of LA wider (tr.) than basal glabellar width. Posterior margin of glabella gently convex posteriorly (Figs. 14.2, 14.6, 17.1) or almost linear (tr.) (Figs. 12.4, 12.6, 17.13). SO deep only abaxially, abaxial end slightly anterior to adaxial end. S1 deepest abaxially, oriented strongly anterolaterally abaxially. LO and L1 subtrapezoidal, narrowing anteriorly; axial furrow very shallow or not incised at lateral margins of L1 (Figs. 12.1, 12.5, 12.6, 14.2, 14.3, 17.13). S2 deepest abaxially, roughly transverse. L2 subrectangular, lateral margins bowing slightly outwards. S3 pit-like, isolated from axial furrow. L3 subtrapezoidal, widening (tr.) anteriorly until contact with ocular lobes. LA hemispherical to transversely oblate, well inflated dorsally above extraocular area, slightly higher than posterior glabellar lobes (Fig. 17.4. 17.7, 17.11, 17.16). Large axial node on LO, smaller axial node occasionally retained on L1 (Fig. 17.13) and rarely on L2 (Fig. 12.5). (Nodes on L1 and L2 more commonly developed on cephala from stratigraphically older collections; Fig. 1.2.) Ocular lobes strongly divergent, crescentic, tip widely separated from glabella, oriented nearly straight posteriorly, posterior tip opposite midlength of L1, convex dorsally; ocular furrow not developed. Interocular area gently arched dorsally (can appear shelf-like on compacted specimens), almost twice width (tr.) of ocular lobes and almost half width (tr.) of extraocular area opposite L2; weak interocular swellings rarely retained on cephala up to 8.3 mm sag. length (Figs. 12.4, 12.7, 14.2, 14.5, 17.17). Posterior ocular line and rarely weak intergenal ridge retained on some individuals (Figs. 12.1, 12.3, 12.4, 12.6, 12.7, 12.9, 14.1, 14.3, 14.6). Weak genal caeca rarely developed (Fig. 12.4) and genal ridge very rarely developed (Fig. 12.6) on extraocular area on cephala >5.9 mm long (sag.). Bertillon markings occasionally developed on LA (Figs. 12.4, 17.1), very rarely passing onto L3 and ocular lobes. Terrace lines on cephalic doublure and genal spines (Fig. 17.1, 17.9, 17.14), occasionally lateral and rarely posterolateral cephalic border (dorsal) (Fig. 17.17).

Mature hypostome (Fig. 13.13–24) with convex, subglobular middle body, less convex at smaller size (Fig. 13.1–12). Anterior marginal flange narrow (sag.), separated from middle body by distinct furrow; anterior wing triangular, approximately one-third distance down hypostomal length on small specimens (Fig. 13.2, 13.6), just posterior to hypostomal midlength on larger specimens (Fig. 13.10, 13.14, 13.18, 13.22). Posterior lobe subrectangular, maximum width approximately two-thirds maximum hypostomal width, length (sag.) almost one-half that of middle body. Furrows separating posterior lobe from middle body deep, absent over axis, oriented strongly posteriorly adaxially. Six pairs of marginal spines plus medial spine around margins of posterior body on small specimens (Fig. 13.1), medial spine lost (leaving slight indentation on posterior margin of posterior body) and paired marginal spines reduced to subtle swellings on larger specimens (Fig. 13.5, 13.9, 13.13, 13.17, 13.21). Bertillon markings on middle body and posterior body (Fig. 13.13, 13.17, 13.21).

Prothorax (Figs. 12.1–3, 14.1–5) of 13 segments; width (tr.) of axis approximately three-quarters width (tr.) of inner pleural region on T1, gently tapering posteriorly. Axial nodes developed on all segments, more prominent or spinelet-like on segments posterior to T8, occasionally also more prominent on T1 and T2 (Figs. 12.7, 14.1). Inner pleural regions of T1 and T2 transverse, tapering distally, with straight margins; pleural spines sentate and divergent. T3 hyperpleural; pleural spine dolichospinous. Inner pleural region of T4 and to lesser extent T5 tapering distally. Inner pleural regions of T6 to T9 transverse, parallel-sided, with straight margins. Inner pleural regions of T10 to T13 increasingly divergent, parallel-sided, margins increasingly curved in more posterior segments. Pleural spines of T4 to T7 or T8 sentate; those of T8 or T9 to T13 increasingly falcate; all divergent, becoming subpendent on posterior segments. Pleural furrows extend onto pleural spines of T3 and T8 or T9 to T13. Pleural spine of T3 may bear a dorsal granular ornament (Fig. 12.2), occasionally coalescing into terrace lines or bertillon markings proximally, ventral surface with terrace lines. Pleural spines of T11 to T13 rarely with weak terrace lines ventrally (Fig. 12.8).

Opisthothorax (Figs. 12.8, 14.1–5, 14.7–9) of at least 32 segments. Axial nodes on T14 to T16, T17, or T18, absent on more posterior segments. Inner pleural regions of T14 and T15 slightly curved, tapering, divergent; becoming straight, parallel-sided, and divergent on more posterior segments; pleural spines of all segments sentate, divergent. Pleural furrow shallow, terminating on inner pleural region, absent on segments posterior to T17-22. Axial furrow shallow or absent on segments posterior to T17, inner pleural region then separated from axis by break in slope only (Fig. 14.7). Rest of opisthothorax and pygidium unknown.

Ontogeny.—Silicified specimens, combined with larger specimens preserved in shale, allow detailed study of the ontogeny of *Nephrolenellus geniculatus* from sag. cephalic lengths of 0.54 mm to approximately 11.8 mm through all four phases of cephalic development.

Phase 1 (Fig. 15.1, 15.2): Observed cephalic lengths range from 0.54 mm to 0.72 mm. Cephalon initially subcircular in outline, posterior cephalic margin straight, roughly transverse. Intergenal spines open ventrally, posteroventrally oriented at approximately 20° from horizontal, proximal portion slightly convergent, distal portion parallel to exsag. axis; length approximately two-thirds of sag. cephalic length. Anterior border gently rounded dorsally, extends around lateral cephalic margin and contacts abaxial margin of intergenal spines; exsagittal length approximately equal to that of LO. Glabella touches wide anterior border furrow, slightly constricted at S3, defined by deep axial furrow, relief prominent. SO, S1, S2, and S3 transverse, deepest distally. LO ovate, exsagittal length one-tenth of sagittal cephalic length. L1, L2, and L3 subcircular, exsagittal length of each one-sixth of sagittal cephalic length. LA subcircular, inflated, summit at same dorsal elevation as more posterior glabellar lobes; sagittal length approximately one-quarter that of cephalon; width slightly greater than that of L1 (tr.). LO, L1, L2, and L3 each with prominent axial node developed centrally, node on LO smallest. Ocular lobes prominent, dorsal surface above level of glabella, arcuate; strongly divergent proximally, bending to run closer to parallel with exsagittal axis opposite posterior third of L3; convex dorsally; width uniform; inflated posteriorly as far as opposite midlength of L1; posterior ocular line extends to abaxial margin of intergenal spines. Ocular lobes contact and run confluent with lateral cephalic border opposite S2. Interocular area shelf-like or very slightly arched dorsally. Pleural extensions of L1, L2, and L3 defined by interocular furrows; each with interocular node developed midway between axial furrow and ocular lobe; summit of interocular nodes as high in relief as glabellar axial nodes. Pleural extension of L1 runs posterolaterally to base of intergenal spines as intergenal ridge.

Morphological changes during phase 1 of cephalic development were very subtle, consisting most obviously of a slight proportional decrease in the distance between the intergenal spine bases relative to sagittal cephalic length (Figs. 2.2, 18.1).

Phase 2 (Fig. 15.3–11): Observed cephalic lengths range from 0.74 mm to 1.03 mm. During this phase, the proportional distance between the intergenal spine bases increased relative to sagittal cephalic length (Figs. 2.2, 18.2), the intergenal spines lengthened (to almost same length as cephalon); the extent of contact between the ocular lobes and the lateral cephalic border decreased until they became separated by a very narrow extraocular area (Fig. 15.11). The ocular lobes inflated into sausage-shaped structures, and the posterior ocular line connecting the posterior tips of the ocular lobes to the outside edge of the intergenal spine was reduced in prominence (Fig. 15.11). Shape change of the glabella was subtle: LA proportionally elongated (sag.) and slightly widened (tr.) at its contact with the anterior margin of the ocular lobes (Fig. 18.2), and the glabella became more markedly constricted at S3.

Statistical comparison of vectors of ontogenetic shape change reveals that the pattern of shape change followed during phase 2 of cephalic development (Fig. 18.2) was significantly different from that followed during phase 1 (Fig. 18.1) using landmark configuration 1 (phase 1, n = 5; phase 2, n = 7; between-phase angle of 95.2° based on vectors derived from Bookstein coordinates or 92.1° based on vectors derived from warp scores [reference form = consensus form of smallest 2 cephala in phase 1 of development], both significant at 95% confidence based on bootstrap resampling [400 iterations]), in agreement with results of previous analyses (Webster et al., 2001).

Phase 3 (Fig. 15.12–32): Observed cephalic lengths range from 1.21 mm to 2.82 mm. Cephalon initially horseshoe-shaped to subcircular in outline, posterior cephalic margin straight, angled slightly posteriorly abaxially. Genal spines present as small bud-like extensions of the lateral cephalic border, located immediately

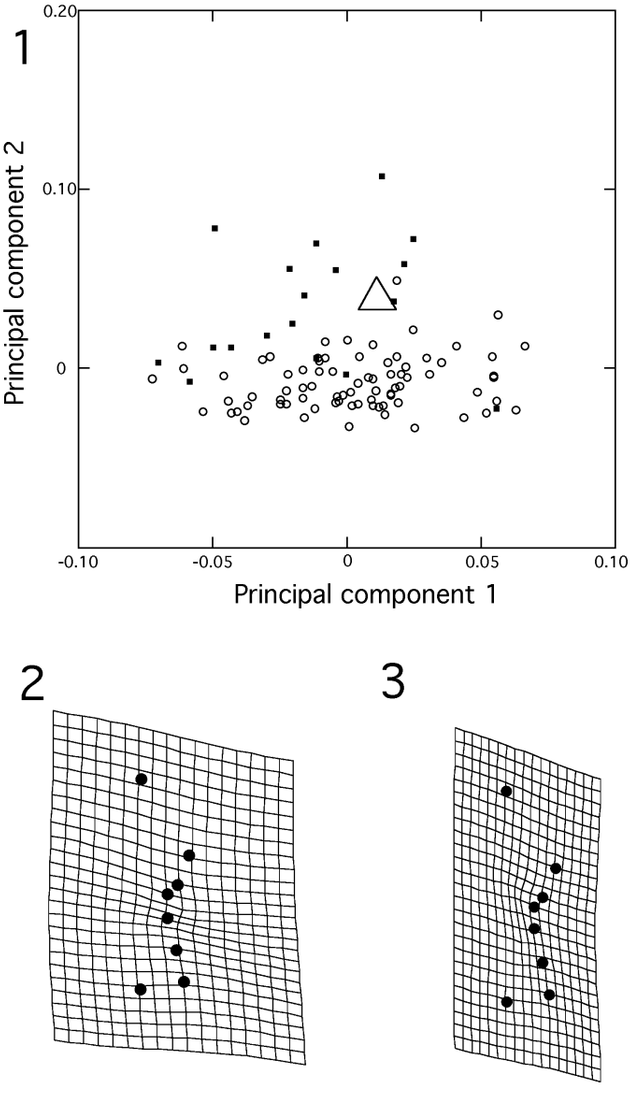

FIGURE *11—1*, Summary of a geometric morphometric analysis of varation in glabellar shape on cephala in phase 4 of development of *Nephrolenellus multinodus* from the Great Basin (squares), *N. geniculatus* (circles), and GSC 16858 (triangle). Warp scores (consisting of two uniform terms plus x- and y-components of the five partial warps) were calculated for the glabellar landmark configuration (configuration 4, Fig. 4) of all specimens (using the mean form of all specimens as the reference form), and were subjected to a principal component analysis. Specimen scores on the first two resulting principal components (summarizing 37% and 25% of the total variance in the data set, respectively) reveal subtle differences in glabellar morphology between *N. multinodus* and *N. geniculatus*, as seen by their separation in morphospace (see text). GSC 16858 falls within the bounds of variation expressed by *N. multinodus* from the Great Basin (on these and all higher PCs), supporting its assignment to this species (see text). *2*, Thin-plate spline deformation grid depicting the nature of shape change described by the first principal component (predominantly a longitudinal shortening of L2 from low to high scores, likely corresponding to a general ontogenetic trend). *3*, Thin-plate spline deformation grid depicting the nature of shape change described by the second principal component (predominantly a transverse narrowing of L2 from high to low scores, corresponding to a phylogenetic difference between *N. multinodus* and *N. geniculatus*).

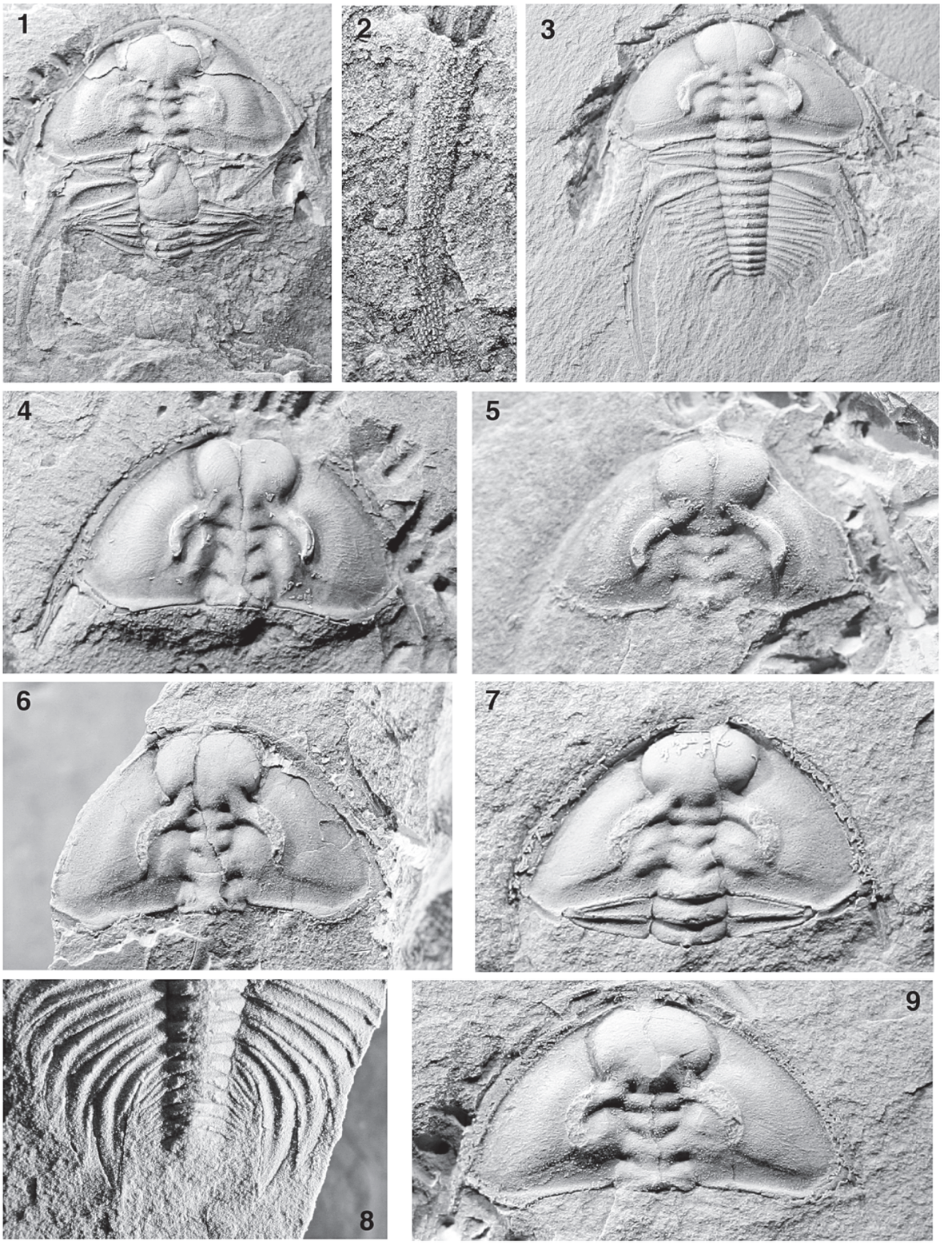

FIGURE *12*—*Nephrolenellus geniculatus* in late phase 4 of cephalic development. *1, 2*, Partial articulated exoskeleton in molt configuration, with hypostome and rostral plate rotated 180° ventrally (pivoting near the base of the genal spines) relative to life position and now visible upside-down and pointing posteriorly down the thorax on the internal mold, CMCP 2325. *1,* Entire specimen, ×3; *2*, Details of granular ornament on left pleural spine of T3, ×10. *3,* Partial articulated exoskeleton, FMNH PE57994, ×4. *4*, Cephalon showing extraocular genal caeca, FMNH PE57995, ×4. *5*, Cephalon showing axial nodes on LO, L1, and L2, FMNH 57996, ×5. *6,* Cephalon showing ornament including weak genal ridge, FMNH 57747, ×4. *7*, Cephalon and anterior prothorax, FMNH PE57997, ×5. *8,* Details of posterior prothorax and opisthothorax showing faint terrace lines on impression of doublure on right pleural spines of T11–T13 (posteriormost segments of prothorax), FMNH PE57998, ×7. *9*, Cephalon FMNH PE57999, ×5. All specimens are dorsal views of internal molds from ICS-1044, Ruin Wash section, Chief Range, Nevada. See text for stratigraphic details.

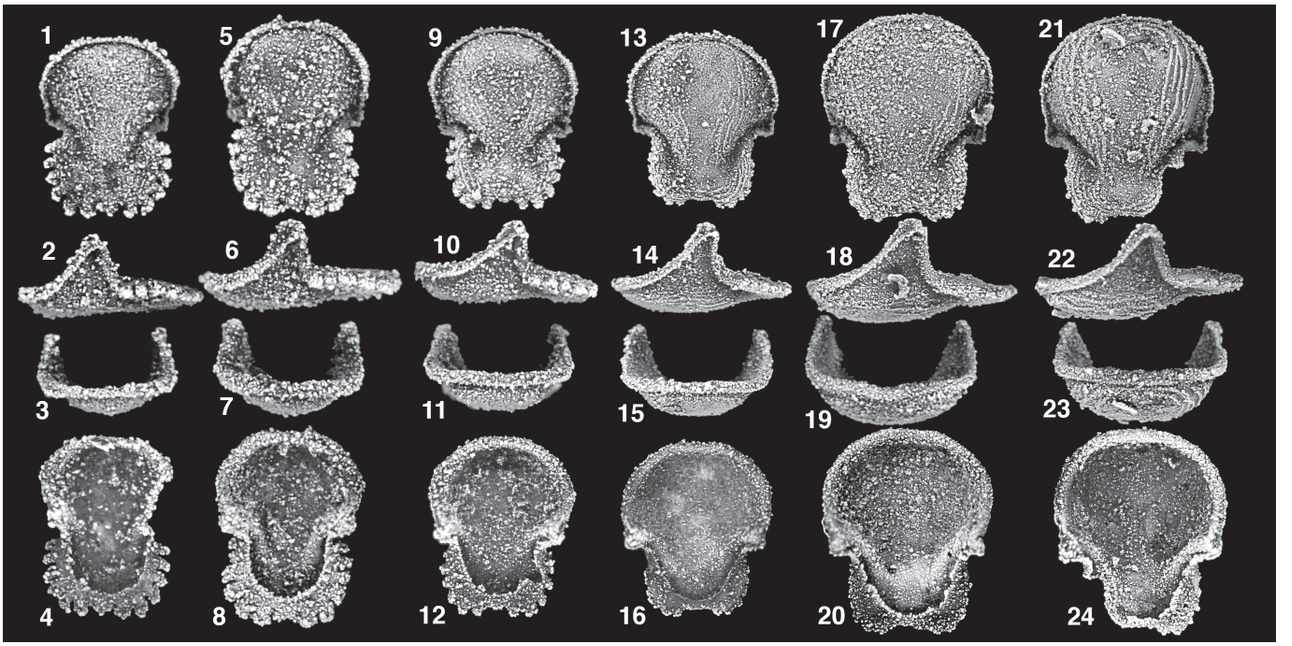

FIGURE *13*—Ontogenetic development of the hypostome of *Nephrolenellus geniculatus*, larger specimens to the right. *1–4*, Small hypostome in ventral, left lateral, anterior, and dorsal views, FMNH PE57947, ×18. *5–8*, FMNH PE57949 in ventral, left lateral, anterior, and dorsal views, ×16. *9–12*, FMNH PE57951 in ventral, left lateral, anterior, and dorsal views, ×12. *13–16*, FMNH PE57952 in ventral, left lateral, anterior, and dorsal views, ×10. *17–20*, FMNH PE57954 in ventral, left lateral, anterior, and dorsal views, ×9. *21–24*, FMNH PE57955 in ventral, right lateral, anterior, and dorsal views, ×8. The right lateral view has been computationally reflected for consistency with views of other specimens. All specimens from ICS-1173, Hidden Valley section, Burnt Springs Range, Nevada. See text for stratigraphic details.

lateral (and slightly ventral) to base of intergenal spines. Intergenal spines open ventrally (Fig. 15.13), dipping ventrally at approximately 5° relative to rest of cephalon; length at least half that of cephalon (sag.). Cephalic border well defined around entire cephalon by distinct border furrow; gently rounded dorsally anteriorly; width of anterior border opposite junction of ocular lobes with LA approximately equal to length (exsag.) of LO. Glabella constricted at S3, defined by deep axial furrow. SO, S1, S2, and S3 transverse, deepest distally. LO transversely ovate, length (exsag.) approximately one-tenth of sag. cephalic length; slightly wider than L1. L1, L2, and L3 subrectangular, successively narrowing slightly anteriorly; L3 slightly shorter (sag.) than L1 or L2. LA subcircular, inflated, summit at same dorsal elevation as more posterior glabellar lobes (Fig. 15.14); sagittal length approximately one-third that of cephalon; maximum width slightly wider than that of LO (tr.). LO, L1, L2, and L3 each with axial node developed centrally, node on L3 smallest. Ocular lobes prominent, bulbous, convex dorsally, widest opposite anterior third of L2, dorsal surface above level of glabella (Fig. 15.15), crescentic; strongly divergent proximally, bending to run almost parallel with exsagittal axis opposite midlength of L2; posterior tip opposite L1. Interocular area shelf-like. Pleural extensions of L1, L2, and L3 defined by interocular furrows; each with interocular node developed midway between axial furrow and ocular lobe, node opposite L3 weak; summit of interocular nodes subdued below relief of glabellar axial nodes. Pleural extension of L1 runs posterolaterally to base of intergenal spines as intergenal ridge. Posterior ocular line weak.

Considerable morphological change occurred during phase 3 of cephalic development (Fig. 18.3). The extraocular area continued to widen, the posterior cephalic margin elongated, and a weak adgenal angle developed just adaxial to the base of the intergenal spine (Fig. 15.19, 15.23, 15.26, 15.30). The genal spines elongated, such that they are stubby, blunt, structures approximately twice as long as LO (exsag.) slightly separated from the intergenal spines on cephala in late phase 3 of development (Fig. 15.26, 15.30). The intergenal spines became more posterolaterally directed and proportionally shortened, being considerably less than half the length of the cephalon on mid phase 3 cephala (Fig. 15.26) and reduced to small spines or nubs on late phase 3 cephala (Fig. 15.30); they are virtually closed ventrally on late phase 3 cephala. LO proportionally widened and lengthened, such that the glabella tapers evenly anteriorly to L2 or S3 on late phase 3 cephala. L3 proportionally shortened (exsag.) and widened (tr.), increasing its extent of contact with the adaxial margin of the ocular lobes. LA continued to increase in proportional size and abutted strongly against the anterior cephalic border on late phase 3 cephala (Fig. 15.30–31). On late phase 3 cephala LA is dorsally inflated above the level of more posterior glabellar lobes and is wider (tr.) than LO (Fig. 15.30–31). An anterior arch is present on cephala in late phase 3 of development, although it is subdued somewhat by deflection of the anterior cephalic border associated with inflation of LA (contrast Fig. 15.15, 15.17, 15.22, 15.25, 15.28, 15.32). The glabella became more constricted at L2 as this lobe continued to proportionally narrow. Axial nodes on L3 and L2 are typically absent on large phase 3 cephala, the node on L1 is reduced in size, the node on LO is more spine-like, and the interocular nodes are subdued or even absent (Fig. 15.26), although interocular furrows can remain as shallow depressions. The ocular lobes are of mature morphology, and the posterior ocular line and intergenal ridge are much reduced in prominence (or may even be absent) relative to ontogenetically younger cephala (Fig. 15.23, 15.26). Terrace lines on the cephalic doublure and ventral surface of the genal spines first become visible on cephala in phase 3 of development (Fig. 15.20–22, 15.27–29).

Specimens in phase 3 of cephalic development with sag. cephalic lengths 2.2 mm and 2.8 mm possess 10 and 12 prothoracic segments respectively (opisthothorax, if present, and pygidium not preserved in either case). All preserved aspects of the thoraxes

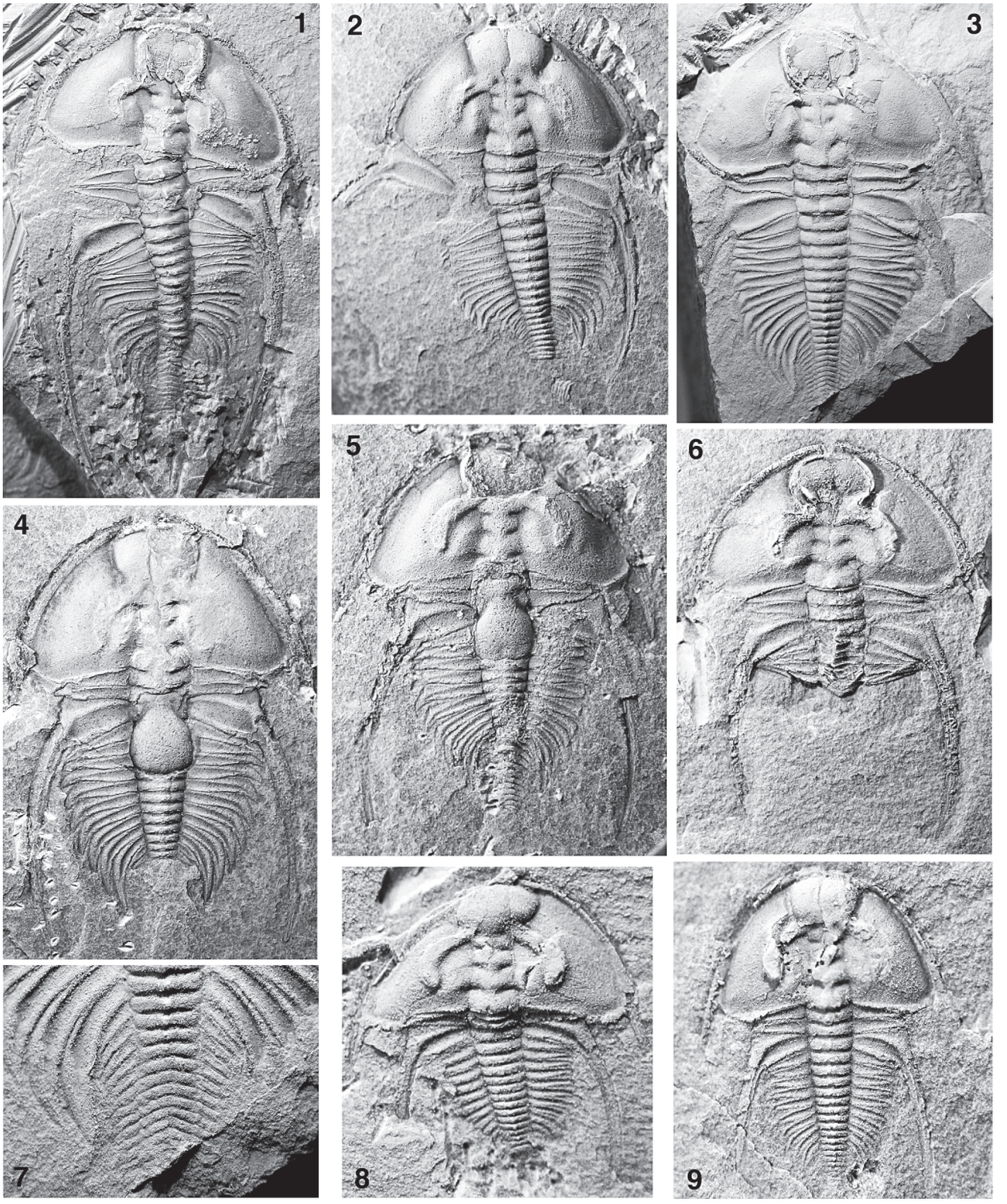

FIGURE *14*—Articulated specimens of *Nephrolenellus geniculatus* in phase 4 of cephalic development showing details of the prothorax and opisthothorax. *1*, Almost complete dorsal exoskeleton showing slight disarticulation of thorax and separation of some thoracic pleurae from axial rings, hypostome in place, FMNH PE57942, ×3. *2*, Almost complete dorsal exoskeleton showing disarticulation of the thorax at the T3–T4 joint and in the opisthothorax, and separation of T3 pleurae from the axial ring, UCR 9945.111, ×4. *3, 7*, Internal mold of holotype, FMNH PE57943. *3*, Almost complete dorsal exoskeleton, hypostome in place, ×2.5; *7*, details of opisthothorax, ×6. *4, 5*, Articulated exoskeletons in molt configuration, with hypostome and rostral plate rotated 180° ventrally (pivoting at the base of the genal spines) relative to life position and now visible upside-down and pointing posteriorly down the thorax on the internal mold. *4*, UCR 9945.126, ×4; *5*, FMNH PE57434, ×6. *6*, "Enrolled" exoskeleton, with posterior portion of prothorax flipped below anterior portion, hypostome in place, FMNH PE57944, ×5. *8, 9*, Small articulated specimens in early phase 4 of cephalic development. *8*, FMNH PE57945, ×8; *9*, FMNH PE57946, ×8. All specimens are dorsal views of internal molds from ICS-1044, Ruin Wash section, Chief Range, Nevada. See text for stratigraphic details.

are similar to the condition seen on specimens with cephalic lengths >5 mm (described above).

A statistical comparison of vectors of ontogenetic shape change determined that the pattern of shape change followed during phase 3 of cephalic development (Fig. 18.3) was significantly different from that followed during phase 2 (Fig. 18.2) using landmark configuration 2 (phase 2, n = 7; phase 3, n = 13; between-phase angle of 71.8° based on vectors derived from Bookstein coordinates or 69.2° based on vectors derived from warp scores [reference form = consensus form of smallest 2 cephala in phase 2 of development], both significant at 95% confidence based on bootstrap resampling [400 iterations]), in agreement with results of previous analyses (Webster et al., 2001).

Phase 4 (Figs. 16, 17, 12, 14): Observed cephalic lengths range from 3.19 mm to approximately 11.8 mm. Cephalon initially semicircular in outline, proximal portion of posterior cephalic margin angled slightly posteriorly abaxially, distal portion deflected anteriorly at adgenal angle located approximately midway along posterior cephalic margin. Genal spines slender, just over one-quarter of sagittal cephalic length, base developed opposite (Fig. 16.1) or slightly posterior to LO (Fig. 16.4). Intergenal spines or nubs closed ventrally, cylindrical in cross-section, posterolaterally oriented; length equal to or less than that of LO (exsag.), located two-thirds of distance between adgenal angle and genal spines. Cephalic border well defined around entire cephalon by distinct border furrow; rounded dorsally anteriorly; width of anterior border opposite junction of ocular lobes with LA approximately half length (exsag.) of LO; posterior border narrows adaxially. Glabella constricted at L2. Maximum width of LA wider (tr.) than basal glabellar width. Posterior margin of glabella very gently convex posteriorly or transverse. SO deep only abaxially, roughly transverse. S1 and S2 deepest abaxially, roughly transverse. LO and L1 subtrapezoidal, narrowing anteriorly; axial furrow shallow at lateral margins of L1. L2 subrectangular, lateral margins bowing slightly outwards. S3 very shallow axially and along contact between L3 and ocular lobes, deepest in pit-like position midway between axial furrow and sagittal axis. L3 subtrapezoidal, widening (tr.) anteriorly until contact with ocular lobes. LA hemispherical to transversely oblate, well inflated dorsally above extraocular area, slightly higher than posterior glabellar lobes (Fig. 16.3, 16.6). Axial node on LO and L1 (occasionally also on L2), decreasing in size anteriorly. Ocular lobes strongly divergent, crescentic, tip widely separated from glabella, oriented nearly straight posteriorly, posterior tip opposite L1, convex dorsally; ocular furrow not developed. Interocular area shelflike, slightly wider than width (tr.) of ocular lobes and approximately equal to width (tr.) of extraocular area opposite L2; interocular furrows shallow or absent. Posterior ocular line and intergenal ridge weak or absent.

Phase 4 morphology of cephala >5 mm length (sag.) was described above. Morphological changes during early phase 4 (see also Fig. 18.4) include development of a stronger adgenal angle (contrast Figs. 16.1 and 16.4 with Figs. 16.7, 16.10, 16.16, 16.17, 16.20, 16.24, and 17) and continued proportional lateral widening and longitudinal shortening of L3. Very shallow interocular furrows are rarely visible on cephala up to 6.5 mm long (sag.). The interocular area first becomes arched or sloping on cephala approximately 3 mm long (sag.) (e.g., Fig. 16.18). Ornament such as bertillon markings on LA first becomes apparent on cephala 3.2 mm long.

Specimens with sagittal cephalic lengths 3 mm and 3.1 mm possess all 13 prothoracic segments plus 4 and 6 opisthothoracic segments respectively (pygidium not preserved; Fig. 14.8, 14.9). At least 10 opisthothoracic segments are present on a specimen with sagittal cephalic length 4.6 mm (pygidium not preserved). Terrace lines (ventrally), bertillon markings, and granulations on the pleural spine of T3 are evident on specimens with sagittal cephalic lengths 3.1 mm, 3.4 mm, and 3.8 mm respectively.

Using data from silicified specimens only, a statistical comparison of vectors of ontogenetic shape change determined that the pattern of shape change followed during phase 4 of cephalic development (Fig. 18.4) was not significantly different from that followed during phase 3 (Fig. 18.3) (landmark configuration 3; phase 3, n = 10; phase 4, n = 9; between-phase angle of 35.2° based on vectors derived from Bookstein coordinates or 54.8° based on vectors derived from warp scores [reference form = consensus form of 3 smallest cephala in phase 3 of development], neither significant at 95% confidence based on bootstrap resampling [400 iterations]). This conclusion holds when sample size for cephala in phase 4 of development is increased by including data from specimens preserved in shale (landmark configuration 3; phase 3, n = 10; phase 4, n = 26; between-phase angle of 18.5° based on vectors derived from Bookstein coordinates or 24.3° based on vectors derived from warp scores [reference form = consensus form of 3 smallest cephala in phase 3 of development], neither significant at 95% confidence based on bootstrap resampling [400 iterations]) and is in agreement with results from an earlier study (Webster et al., 2001). However, a significant difference in allometric patterning is detected between phase 3 and phase 4 of cephalic development when only landmarks summarizing glabellar morphology are considered (landmark configuration 4; silicified specimens only; phase 3, n = 14; phase 4, n = 16; between-phase angle of 83.3° based on vectors derived from Bookstein coordinates or 66.5° based on vectors derived from warp scores [reference form = consensus form of 2 smallest cephala in phase 1 of development], both significant at 95% confidence based on bootstrap resampling [400 iterations]).

Holotype.—DMNH 16052, designated by Palmer (1998, fig. 6.8). The internal mold of this specimen is FMNH PE57943, illustrated here for the first time (Fig. 14.3, 14.7).

Occurrence.—CALIFORNIA: *Marble Mountains, San Bernardino County:* UCR 9931 (shales 32.99 m to 33.28 m above top of Chambless Limestone cliff), UCR 9933 (shales 33.67 m to 33.72 m above top of Chambless Limestone cliff), UCR 9934 (shales 33.72 to 33.82 m above top of Chambless Limestone cliff); all in the Cadiz Formation. *Eagle Mountain, Inyo County:* Silicified specimens about 4 m above the uppermost occurrence of *N. multinodus* (Fowler, 1999). NEVADA: *Chief Range, Lincoln County:* Ruin Wash section, ICS-1044 and UCR 9945 (shales) (see also Palmer, 1998, 1999a); Klondike Gap section (new collections); all in the uppermost meter of the Combined Metals Member, Pioche Formation. *Antelope Canyon, Lincoln County:* Shales and silicified fauna in carbonate nodules (new collections) from uppermost Combined Metals Member (see also Sundberg and McCollum, 2000). *Burnt Springs Range, Lincoln County:* Hidden Valley section (Fig. 1), ICS-1186, UCR 10226, and UCR 10227 (various horizons from 6.4 m to 2.2 m below ribbon carbonate marking base of Middle Cambrian), ICS-1278 (carbonate nodules 3.2 m below ribbon carbonate marking base of Middle Cambrian), ICS-1277 and ICS-1185 (shale and thin limestone 2.2 m below ribbon carbonate marking base of Middle Cambrian), ICS-1184 (shale 2.0 m to 2.2 m below ribbon carbonate marking base of Middle Cambrian), ICS-1173 and UCR 9963 (carbonate nodules 1.8 m below ribbon carbonate marking base of Middle Cambrian, Palmer, 1998), ICS-1179 (carbonate lens from float above ICS-1173, less than 2 m below ribbon carbonate marking base of Middle Cambrian, Palmer, 1998), ICS-1178 and UCR 10228 (shale 0 m to 1.7 m below ribbon carbonate marking base of Middle Cambrian); all in the Combined Metals Member, Pioche Formation. See also Sundberg and McCollum (2000). *Delamar Mountains, Lincoln County:* Oak Spring Summit section, shales 5.27 m to 0 m below ribbon carbonate marking base of Middle Cambrian (Palmer, 1998, 1999b), and USGS locality 7224-CO (Palmer and Halley, 1979); Grassy Spring section (Palmer, 1998); all in the Combined Metals Member, Pioche Formation. *Groom Range, Lincoln County:* (new collections). ARIZONA: *? Grand Canyon:* Columbine Falls (see Resser in McKee, 1945, pl. 19, fig. 23).

Discussion.—This species is most similar to *Nephrolenellus multinodus*. Differences between the two taxa are detailed below.

EVOLUTION WITHIN *NEPHROLENELLUS*

Nephrolenellus geniculatus and *N. multinodus* are generally very similar trilobites. They show no obvious differences in thoracic morphology (compare Figs. 7 and 14; although the thorax of *N. multinodus* is known from relatively few specimens, all of

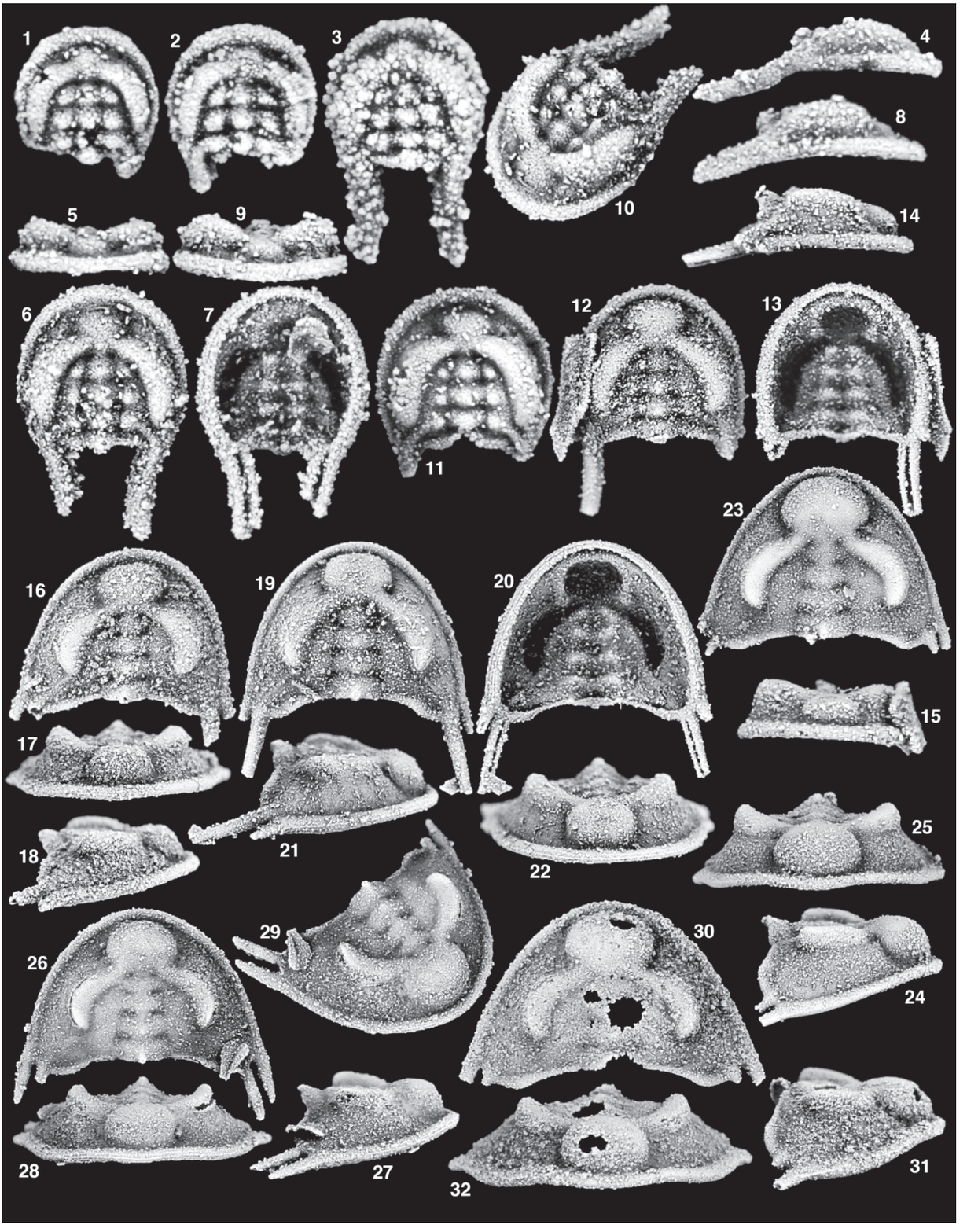

FIGURE *15*—Silicified specimens representing the ontogenetic development of the cephalon of *Nephrolenellus geniculatus* (phases 1 through 3). *1*, Cephalon in phase 1 of development, dorsal view, UCR 9963.191, ×40. Intergenal spines missing. *2*, Cephalon in phase 1 of development, dorsal view, UCR 9963.46, ×40. Intergenal spines missing. *3–5*, Coarsely silicified cephalon in phase 2 of development, dorsal, right lateral, and anterior views, FMNH PE57991, ×37. *6–10*, Cephalon in phase 2 of development, dorsal, ventral, right lateral, anterior, and oblique left anterolateral views, UCR 9963.5, ×35. *11*, Cephalon in phase 2 of development, dorsal view, UCR 9963.190, ×32. Intergenal spines missing. *12–15*, Cephalon in phase 3 of development, dorsal, ventral, right lateral, and anterior views, UCR 9963.10, ×20. Tips of intergenal spines missing. *16–18,* Slightly distorted cephalon in phase 3 of development, dorsal,

which have undergone minor tectonic deformation and are therefore unsuitable for morphometric analysis). The mature hypostome of in *N. multinodus* develops a subtle notch in the anterior marginal flange and retains a prominent medial spine on the posterior body, whereas the hypostome of *N. geniculatus* lacks the notch and progressively loses the median spine during ontogenetic development (compare Figs. 6 and 13; see also Palmer, 1998, figs. 6.6, 6.10). The most obvious differences between the taxa are found on their mature cephala: *N. geniculatus* lacks a preglabellar field throughout ontogeny (although large *N. multinodus* cephala in phase 4 of development lack a preglabellar field), and possesses a stronger adgenal angle and typically fewer axial nodes on the glabella at morphological maturity. The mature glabella of *N. geniculatus* is consistently proportionally narrower at L2 (Fig. 11.1, 11.3). *Nephrolenellus geniculatus* also lacks an axial node on LA at early ontogenetic stages, while such a node is developed on small *N. multinodus* cephala. Given the nature of these interspecific differences, previous studies have focused on cephalic morphology alone when investigating the evolution within the genus (Webster et al., 2001; Webster and Zelditch, 2005). Although not representing the entire organism, such a focus does relate to the vast majority of evolving morphological attributes.

Studying cephalic differences between the species in an ontogenetically dynamic sense reveals a complex array of modifications to morphological development. Both species progressively lose axial nodes from the glabella during ontogeny, with the rate of node loss being significantly higher (relative to cephalic size) in *N. geniculatus* (Webster and Zelditch, 2005, fig. 4). Conversely, the rate of shape change of the glabella and ocular lobes during phases 3 and 4 of cephalic development (relative to size) is significantly higher in *N. multinodus* (Webster and Zelditch, 2005, fig. 5b).

Both species pass through the same four phases of cephalic development during their respective ontogenies, and many general similarities in the patterns of shape change they follow during each phase can be seen (compare Figs. 10 and 18). However, quantitative analysis demonstrates that the patterns of shape change they follow are significantly different from each other during phase 1 (using landmark configuration 1, at 95% confidence using vectors derived from warp scores, at 90% confidence using vectors derived from Bookstein coordinates; see Webster et al., 2001), during phase 2 (using landmark configuration 1; between-species angle 82.9° based on vectors derived from Bookstein coordinates, significant at 95% confidence based on bootstrap resampling [400 iterations]; vectors derived from warp scores statistically indistinguishable at 95% confidence based on bootstrap resampling [400 iterations]), and during phase 3 (using landmark configuration 3 [Webster et al., 2001]; using landmark configuration 4 [between-species angle 20.6° based on vectors derived from Bookstein coordinates or 25.9° based on vectors derived from warp scores [reference form = consensus form of second instar of *N. multinodus* in phase 1 of development], both significant at 95% confidence based on bootstrap resampling [400 iterations]; or using landmarks summarizing oculo-glabellar morphology [Webster and Zelditch, 2005]). Patterns of ontogenetic shape change followed by the two are statistically indistinguishable from each other during phase 4 (using all 13 landmarks of Fig. 4 [Webster et al., 2001] or using oculo-glabellar landmarks [Webster and Zelditch, 2005]), although taphonomic overprint on observed morphology is an issue (see above).

Interspecific differences in pattern of shape change during phase 1 of cephalic development are very subtle (perhaps accounting for the sensitivity of the inference of significance to morphometric method employed), and seem to relate to a slight narrowing of the glabella at S3 and the posterior margin of LO in *N. multinodus* (see Webster et al., 2001, fig. 4.8a) which is not detected in *N. geniculatus* (Fig. 18.1). Interspecific differences in pattern of shape change during phase 2 of cephalic development chiefly relate to a more pronounced longitudinal elongation and lateral expansion of LA in *N. geniculatus* (Fig. 18.2) relative to *N. multinodus* (Fig. 10.1). The significant difference between the species during phase 2 of cephalic development recovered here (based on vectors derived from warp scores) was not recovered in an earlier analysis based on smaller sample size (Webster et al., 2001). During phase 3 of development *N. multinodus* underwent a more pronounced proportional expansion of LA and correlative shortening (exsag.) and widening (tr.) of L3 (Fig. 10.2) than did *N. geniculatus* (Fig. 18.3), while in the latter species the slight progressive constriction at L2 is more pronounced than in the former taxon.

The species therefore follow unique ontogenetic trajectories of shape change, which ultimately account for the observed differences in mature cephalic morphology. Such complex and mosaic differences in morphological development suggest that the underlying evolutionary modifications to developmental morphogenetic processes were far from simple (discussed by Webster et al., 2001; Webster and Zelditch, 2005).

Cladistic analysis strongly supports a sister-species relationship between the two taxa (Webster et al., 2001). The question remains as to whether the differences in morphological development and mature morphology of *Nephrolenellus multinodus* and *N. geniculatus* resulted from divergence from a common ancestor (as yet undiscovered), or whether *N. multinodus* was directly ancestral to *N. geniculatus*. If the latter is the case, then the interspecific differences in morphological development can be directly interpreted as having resulted from evolutionary modification to the ontogeny of *N. multinodus*. Stratigraphic data are consistent with a hypothesis of direct ancestry: the two species have been recovered from many of the same localities but are not known to stratigraphically co-occur, and *N. multinodus* is consistently the older taxon (Fig. 1; above). It is also of interest that the stratigraphically lowest samples of *N. geniculatus* contain a higher proportion of mature cephala retaining an axial node on L1 and often L2 in addition to the node on LO, in contrast to the stratigraphically higher samples of *N. geniculatus* in which cephala retaining such nodes are far less frequent. This stratigraphic trend (seen at Hidden Valley [Fig. 1], Grassy Spring, the Groom Range, and sections in Death Valley) is consistent with a hypothesis of an evolutionary trend of increased rate of node loss from a *N. multinodus*-like ancestral condition. (The stratigraphically low forms of *N. geniculatus* are otherwise typical of the species in cephalic morphology; silicified material is unavailable, however, and all descriptions and morphometric analyses presented above are based only on the stratigraphically higher material.)

However, a strong case for direct ancestry cannot be made unless it is determined that the purported ancestral taxon lacks autapomorphies, since the acquisition of a derived state in a nodal taxon followed by immediate reversal in the supposed descendant is less parsimonious than the unique acquisition of a derived character state in one terminal taxon. In this light, the presence of a

←

anterior, and right lateral views, UCR 9963.12, ×15. *19–22,* Cephalon in phase 3 of development, dorsal, ventral, right lateral, and anterior views, UCR 9963.13, ×25. Tips of intergenal spines missing. *23–25,* Cephalon in phase 3 of development, dorsal, right lateral, and anterior views, UCR 9963.14, ×12. Tips of intergenal and genal spines missing. *26–29*, Cephalon in phase 3 of development, dorsal, right lateral, anterior, and oblique right anterolateral views, UCR 9963.15, ×11. Tip of left intergenal spine missing. *30–32*, Coarsely silicified and damaged cephalon in late phase 3 of development, dorsal, right lateral, and anterior views, UCR 9963.16, ×12. All specimens from ICS-1173, Hidden Valley section, Burnt Springs Range, Nevada. See text for stratigraphic details.

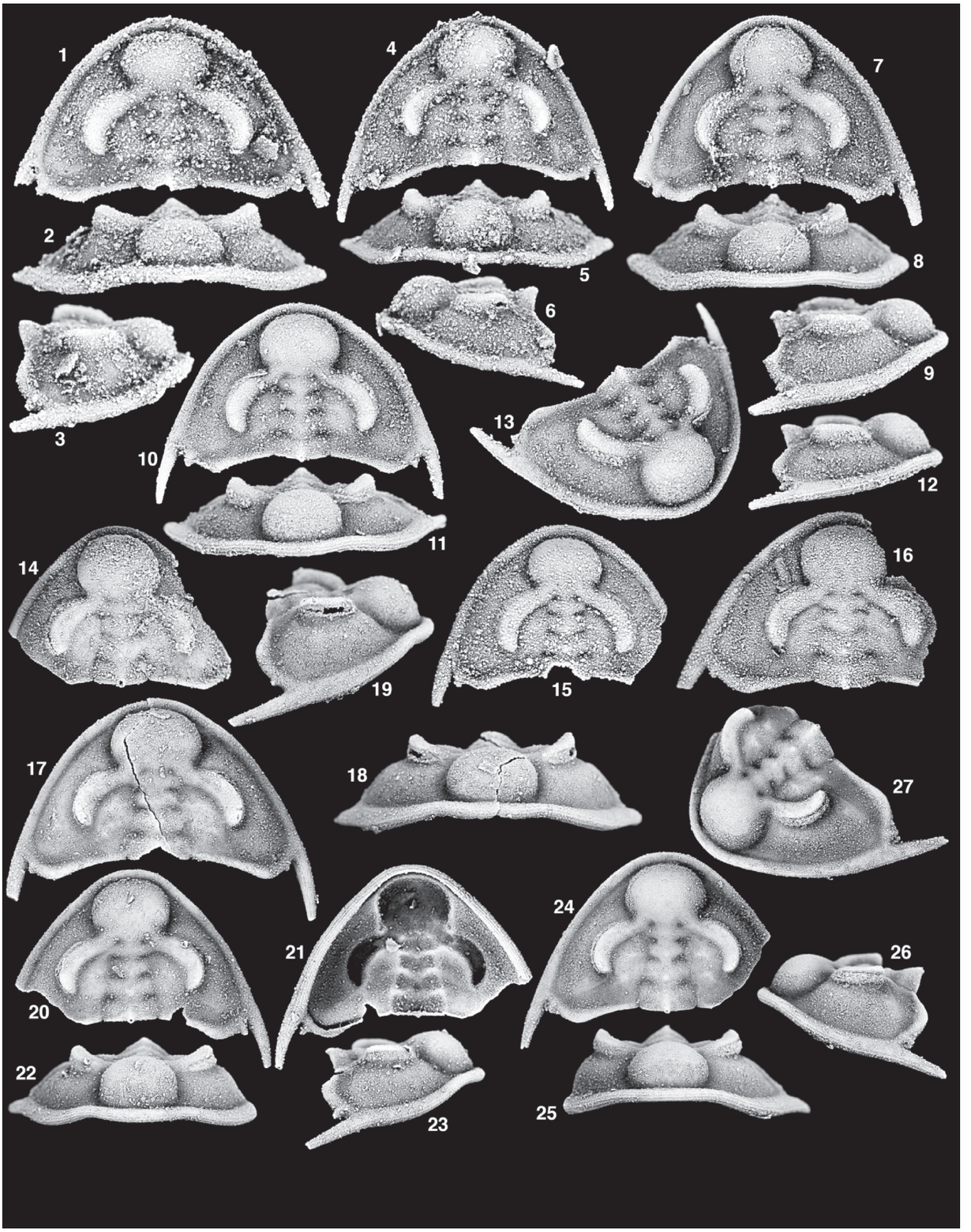

FIGURE *16*—Silicified specimens representing the ontogenetic development of the cephalon of *Nephrolenellus geniculatus* (phase 4). *1–3*, Coarsely silicified cephalon, dorsal, anterior, and right lateral views, UCR 9963.17, ×10. Tip of left genal spine missing. *4–6*, Coarsely silicified cephalon, dorsal, anterior, and left lateral views, UCR 9963.18, ×8. *7–9*, Cephalon, dorsal, anterior, and right lateral views, UCR 9963.21, ×8. Left genal spine missing. *10–13*, Cephalon, dorsal, anterior, right lateral, and oblique right anterolateral views, UCR 9963.19, ×8. *14*, Incomplete cephalon, dorsal view, FMNH PE57956, ×8. *15,* Incomplete cephalon, dorsal view, FMNH PE57966, ×8. *16,* Incomplete cephalon, dorsal view, FMNH PE57962, ×8. *17–19*, Fractured cephalon, dorsal, anterior, and right lateral views, FMNH PE57971, ×7. *20–23*, Incomplete cephalon, dorsal, ventral, anterior, and right lateral views, FMNH PE57972, ×6. *24–27*, Incomplete cephalon, dorsal, anterior, and left lateral views, FMNH PE57973, ×6. All specimens from ICS-1173, Hidden Valley section, Burnt Springs Range, Nevada. See text for stratigraphic details.

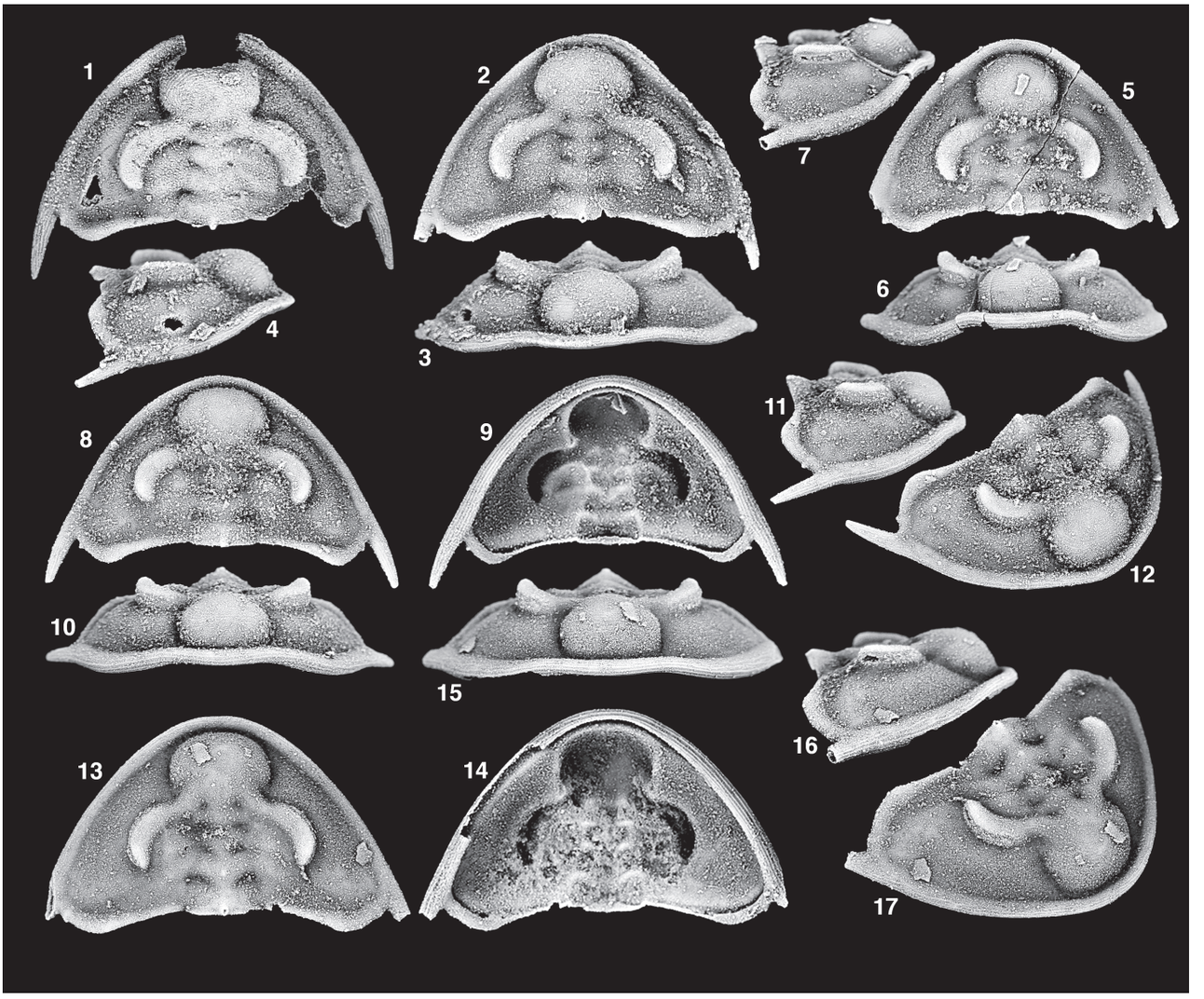

FIGURE *17*—Silicified specimens representing the ontogenetic development of the cephalon of *Nephrolenellus geniculatus* (phase 4). *1*, Incomplete cephalon, dorsal view, FMNH PE57974, ×6. *2–4*, Cephalon, dorsal, anterior, and right lateral views, FMNH PE57975, ×6. *5–7*, Fractured cephalon, dorsal, anterior, and right lateral views, FMNH PE57976, ×5. *8–12*, Coarsely silicified cephalon, dorsal, ventral, anterior, right lateral, and oblique right anterolateral views, FMNH PE57977, ×5. *13–17,* Cephalon, dorsal, ventral, anterior, right lateral, and oblique right anterolateral views, FMNH PE57978, ×5. Tips of genal spines missing. All specimens from ICS-1173, Hidden Valley section, Burnt Springs Range, Nevada. See text for stratigraphic details.

preglabellar field (character 11, state 1) at morphological maturity was unique to *N. multinodus* among the taxa included in the cladistic analysis presented by Webster et al. (2001), and such an apparent autapomorphy would refute a direct ancestor-descendant relationship between it and *N. geniculatus*. However, a preglabellar field is retained at morphological maturity in several closely related taxa not included in the previous cladistic analysis, for example *Bristolia mohavensis* (Crickmay in Hazzard, 1933), the stratigraphically oldest member of the *Bristolia* Harrington, 1956 clade, and *Arcuolenellus arcuatus* (Palmer in Palmer and Halley, 1979), type species of the probable immediate sister-clade to *Nephrolenellus*. The smallest known cephalon of "*Nephrolenellus*? n. sp." (described and assigned to a new genus elsewhere [Webster, in press], see above) has a sagittal length of approximately 6 mm, and it is unknown whether the absence of a preglabellar field at this relatively large size is primary or secondary. A cephalon of another undescribed species of this new genus is approximately 2.4 mm in sagittal length and probably possessed a preglabellar field (based on extrapolation of the curvature of the anterior cephalic border: the specimen is unfortunately incomplete immediately anterior to LA). Furthermore, ontogenetic loss of a preglabellar field over the early portion of cephalic development is known to have occurred in several species of *Bristolia*, *Bolbolenellus*, and *Arcuolenellus* (to be documented elsewhere). Thus, the presence of a preglabellar field in early ontogenetic stages is common to a diverse clade which includes *Nephrolenellus* (and is likely to be plesiomorphic within that genus); and the absence of a preglabellar field at all ontogenetic stages is apparently autapomorphic to *N. geniculatus*. Whether retention of the preglabellar field at relatively large cephalic size in *N. multinodus* is autapomorphic remains ambiguous, pending firm establishment of hypotheses of relationship among the various species mentioned above and *Nephrolenellus*. Similarly, the presence of an axial node on LA at early ontogenetic stages is a potential autapomorphy of *N. multinodus*, or loss of such a node may be apomorphic to *N. geniculatus*: resolution of this ambiguity requires discovery of cephala of *Bristolia*, *Bolbolenellus*, *Arcuolenellus*, and the new genus in early ontogenetic stages. Pending

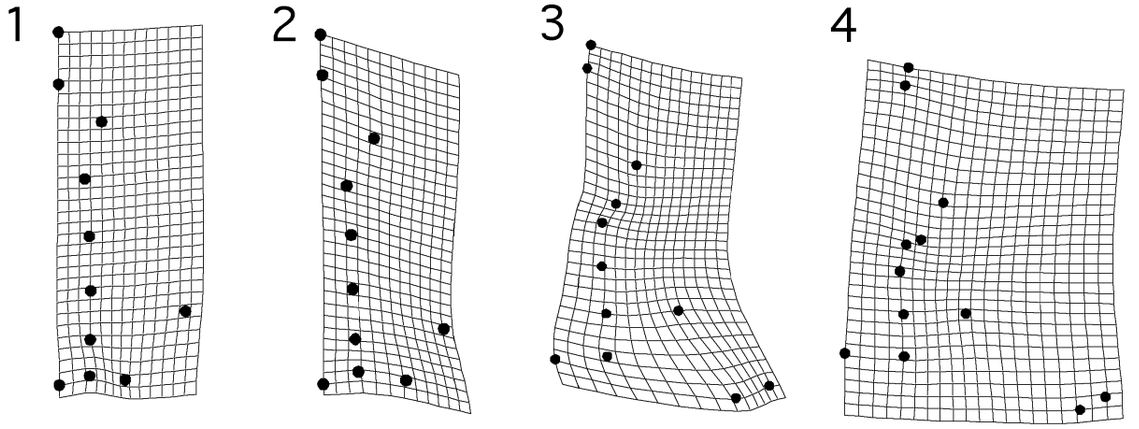

FIGURE *18*—Thin-plate spline deformation grids depicting patterns of shape change during successive phases of cephalic development in *Nephrolenellus geniculatus*. *1,* Phase 1 of cephalic development, landmark configuration 1. *2*, Phase 2 of cephalic development, landmark configuration 1. *3*, Phase 3 of cephalic development, landmark configuration 3. *4*, Phase 4 of cephalic development, landmark configuration 3. See Fig. 4 for details of landmark configurations.

such discoveries, a direct ancestor-descendant relationship between *N. multinodus* and *N. geniculatus*, while possible, represents a suboptimal hypothesis at present.

ACKNOWLEDGMENTS

Thanks are extended to N. Brown, F. Collier, J. Dougherty, E. Fowler, R. Gaines, C. Gronau, G. Gunderson, the Gunthers, N. C. Hughes, M. A. Kooser, D. Levine, L. B. McCollum, M. McCollum, R. Meyer, A. R. Palmer, G. Pari, P. M. Sadler, F. A. Sundberg, J. Thompson, T. White, and T. Whiteley for assistance in the field, valuable discussion, loan of specimens, and access to museum collections. J. M. Adrain provided assistance and advice with photography of silicified specimens. Reviews by G. D. Edgecombe and C. Crônier helped improve the manuscript. L. K. Webster provided assistance in the field, welcome encouragement, and much needed patience at home during the course of this study. Research was funded in part by NSF grant EAR-9980372.

REFERENCES

ADRAIN, J. M. 2005. Aulacopleurid trilobites from the Upper Ordovician of Virginia. Journal of Paleontology, 79:542–563.

ADRAIN, J. M. AND S. R. WESTROP. 2006. New earliest Ordovician trilobite genus *Millardicurus*: the oldest known hystricurid. Journal of Paleontology, 80:650–671.

BEECHER, C. E. 1895. The larval stages of trilobites. American Geologist, 16: 166–197.

BOHACH, L. L. 1997. Systematics and biostratigraphy of Lower Cambrian trilobites of western Laurentia. Unpublished Ph.D. thesis, University of Victoria, 491 p.

BOOKSTEIN, F. L. 1991. Morphometric Tools for Landmark Data: Geometry and Biology. Cambridge University Press, New York, 435 p.

CHATTERTON, B. D. E. AND S. E. SPEYER. 1997. Ontogeny. p. 173–247. *In* R. L. Kaesler (ed.), Treatise on Invertebrate Paleontology, Pt. O, Arthropoda 1, Trilobita, Revised, Volume. 1. Geological Society of America and University of Kansas Press, Lawrence.

CLAUSEN, S. 2004. Paedomorphic patterns of the Cambrian genus *Alueva* (Trilobita, Ellipsocephalidae) from the Iberian Chains (NE Spain). Geobios, 37:336–345.

CRÔNIER, C. AND R. A. FORTEY. 2006. Morphology and ontogeny of an Early Devonian phacopid trilobite with reduced sight from southern Thailand. Journal of Paleontology, 80:529–536.

CRÔNIER, C., R. FEIST, AND J.-C. AUFFREY. 2004. Variation in the eye of *Acuticryphops* (Phacopina, Trilobita) and its evolutionary significance: a biometric and morphometric approach. Paleobiology, 30:471–481.

DRYDEN, I. L. AND K. V. MARDIA. 1998. Statistical Shape Analysis. John Wiley and Sons, New York, 347 p.

EMMONS, E. 1844. The Taconic System; based on observations in New-York, Massachusetts, Maine, Vermont and Rhode-Island. Carroll and Cooke, Printers, Albany, New York.

FORTEY, R. A. 2001. Trilobite systematics: The last 75 years. Journal of Paleontology, 75:1141–1151.

FORTEY, R. A. AND R. M. OWENS. 1997. Evolutionary history, p. 249–287. *In* R. L. Kaesler (ed.), Treatise on Invertebrate Paleontology. Pt. O. Arthropoda 1. Trilobita, Revised. Volume. 1. Geological Society of America and University of Kansas Press, Lawrence.

FORTEY, R. A. AND H. B. WHITTINGTON. 1989. The Trilobita as a natural group. Historical Biology, 2:125–138.

FOWLER, E. 1999. Biostratigraphy of upper Dyeran strata of the Carrara Formation, Emigrant Pass, Nopah Range, California, p. 46–50. *In* A. R. Palmer (ed.), Laurentia 99: V Field Conference of the Cambrian Stage Subdivision Working Group. International Subcommission on Cambrian Stratigraphy. Utah, Nevada, California, U.S.A., September 12–22, 1999. Institute for Cambrian Studies, Boulder, Colorado.

FUSCO, G., N. C. HUGHES, M. WEBSTER, AND A. MINELLI. 2004. Exploring developmental modes in a fossil arthropod: growth and trunk segmentation of the trilobite *Aulacopleura konincki*. American Naturalist, 163:167–183.

HARRINGTON, H. J. 1956. Olenellidae with advanced cephalic spines. Journal of Paleontology, 30:56–61.

HAZZARD, J. C. 1933. Notes on the Cambrian rocks of the eastern Mohave Desert, California. Bulletin of the Department of Geological Sciences, University of California, 23:57–80.

HUGHES, N. C. 1994. Ontogeny, intraspecific variation, and systematics of the Late Cambrian trilobite *Dikelocephalus*. Smithsonian Contributions to Paleobiology, 79. 89p.

HUGHES, N. C. 2003. Trilobite tagmosis and body patterning from morphological and developmental perspectives. Integrative and Comparative Biology, 43:185–206.

HUGHES, N. C. AND R. E. CHAPMAN. 1995. Growth and variation in the Silurian proetide trilobite *Aulacopleura konincki* and its implications for trilobite palaeobiology. Lethaia, 28:333–353.

HUGHES, N. C., R. E. CHAPMAN, AND J. M. ADRAIN. 1999. The stability of thoracic segmentation in trilobites: a case study in developmental and ecological constraints. Evolution and Development, 1:24–35.

HUNT, G. AND R. E. CHAPMAN. 2001. Evaluating hypotheses of instar-grouping in arthropods: a maximum likelihood approach. Paleobiology, 27:466–484.

JELL, P. A. 2003. Phylogeny of Early Cambrian trilobites. Special Papers in Palaeontology, 70:45–57.

KIM, K., H. D. SHEETS, R. A. HANEY, AND C. E. MITCHELL. 2002. Morphometric analysis of ontogeny and allometry of the Middle Ordovician trilobite *Triarthrus becki*. Paleobiology, 28:364–377.

LAUTERBACH, VON K.-E. 1983. Synapomorphien zwischen Trilobiten- und Cheliceratenzweig der Arachnata. Zool. Anz., Jena, 210:213–238.

LIEBERMAN, B. S. 1998. Cladistic analysis of the Early Cambrian olenelloid trilobites. Journal of Paleontology, 72:59–78.

LIEBERMAN, B. S. 1999. Systematic revision of the Olenelloidea (Trilobita, Cambrian). Bulletin of the Peabody Museum of Natural History, Yale University, 35:1–150.

LIEBERMAN, B. S. 2001. Phylogenetic analysis of the Olenellina Walcott, 1890 (Trilobita, Cambrian). Journal of Paleontology, 75:96–115.

LIEBERMAN, B. S. 2002. Phylogenetic analysis of some basal Early Cambrian trilobites, the biogeographic origins of the Eutrilobita, and the timing of the Cambrian Radiation. Journal of Paleontology, 76:692–708.

LIEBERMAN, B. S. 2003. Biogeography of the Trilobita during the Cambrian

radiation: deducing geological processes from trilobite evolution. Special Papers in Palaeontology, 70:59–72.

LOCHMAN, C. 1952. Trilobites, p. 60–184. *In* G. A. Cooper, A. R. V. Arellano, J. H. Johnson, V. J. Okulitch, A. Stoyanow, and C. Lochman (eds.), Cambrian stratigraphy and paleontology near Caborca, northwestern Sonora, Mexico. Smithsonian Miscellaneous Collections, 119 (1).

LONGWELL, C. R. 1928. Geology of the Muddy Mountains, Nevada, with a section through the Virgin Range to the Grand Wash Cliffs, Arizona. U. S. Geological Survey Bulletin 798, 152 p.

MATHWORKS. 2000. MATLAB6. The Mathworks, Natick, Massachusetts.

MCCORMICK, T. AND R. A. FORTEY. 1999. The most widely distributed trilobite species: Ordovician *Carolinites genacinaca*. Journal of Paleontology, 73:202–218.

MCCORMICK, T. AND R. A. FORTEY. 2002. The Ordovician trilobite *Carolinites*, a test case for microevolution in a macrofossil lineage. Palaeontology, 45:229–257.

MCKEE, E. D. 1945. Cambrian history of the Grand Canyon Region. Carnegie Institution of Washington Publication, 563. 232 p.

MCLAIN, D. H. 1974. Drawing contours from arbitrary data points. The Computer Journal, 17:318–324.

MCNAMARA, K. J. 1986. The role of heterochrony in the evolution of Cambrian trilobites. Biological Reviews, 61:121–156.

MOUNTJOY, E. W. 1962. Mount Robson (southeast) map-area, Rocky Mountains of Alberta and British Columbia (83E SE). Geological Survey of Canada, Paper 61-31.

NORFORD, B. S. 1962. Illustrations of Canadian fossils—Cambrian, Ordovician and Silurian of the western Cordillera. Geological Survey of Canada, Paper 62-14:1–25.

PACK, P. D. AND H. B. GAYLE. 1971. A new olenellid trilobite, *Biceratops nevadensis*, from the Lower Cambrian near Las Vegas, Nevada. Journal of Paleontology, 45:893–898.

PALMER, A. R. 1957. Ontogenetic development of two olenellid trilobites. Journal of Paleontology, 31:105–128.

PALMER, A. R. 1998. Terminal Early Cambrian extinction of the Olenellina: Documentation from the Pioche Formation, Nevada. Journal of Paleontology, 72:650–672.

PALMER, A. R. 1999a. Ruin Wash, Chief Range, Nevada, p. 24–25. *In* A. R. Palmer (ed.), Laurentia 99. V Field Conference of the Cambrian Stage Subdivision Working Group, International Subcommision on Cambrian Stratigraphy, Utah, Nevada, California, U.S.A., September 12–22, 1999. Institute for Cambrian Studies, Boulder, Colorado.

PALMER, A. R. 1999b. Oak Springs Summit section, type locality for the base of the Delamaran Stage, p. 26–28. *In* A. R. Palmer (ed.), Laurentia 99. V Field Conference of the Cambrian Stage Subdivision Working Group, International Subcommision on Cambrian Stratigraphy, Utah, Nevada, California, U.S.A., September 12–22, 1999. Institute for Cambrian Studies, Boulder, Colorado.

PALMER, A. R. AND R. B. HALLEY. 1979. Physical stratigraphy and trilobite biostratigraphy of the Carrara Formation (Lower and Middle Cambrian) in the southern Great Basin. U. S. Geological Survey Professional Paper 1047: 1–131.

PALMER, A. R. AND L. N. REPINA. 1993. Through a glass darkly: Taxonomy, phylogeny, and biostratigraphy of the Olenellina. University of Kansas Paleontological Contributions, New Series, 3:1–35.

PALMER, A. R. AND L. N. REPINA. 1997. Suborder Olenellina, p. 405–429. *In* R. L. Kaesler (ed.), Treatise on Invertebrate Paleontology, Pt. O, Arthropoda 1, Trilobita, Revised, Volume 1. Geological Society of America and University of Kansas Press, Lawrence.

PATERSON, J. R. AND G. D. EDGECOMBE. 2006. The Early Cambrian trilobite family Emuellidae Pocock, 1970: systematic position and revision of Australian species. Journal of Paleontology, 80:496–513.

POULSEN, V. 1974. Olenellacean trilobites from eastern North Greenland. Bulletin of the Geological Society of Denmark, 23:79–101.

RAMSKÖLD, L. AND G. D. EDGECOMBE. 1991. Trilobite monophyly revisited. Historical Biology, 4:267–283.

RAW, F. 1925. The development of *Leptoplastus salteri* (Callaway), and of other trilobites (Olenidae, Ptychoparidae, Conocoryphidae, Paradoxidae, Phacopidae, and Mesonacidae). Quarterly Journal of the Geological Society of London, 81:223–324.

RESSER, C. E. 1928. Cambrian fossils from the Mohave Desert. Smithsonian Miscellaneous Collections, 81(2):1–14.

RICHTER, R. 1932. Crustacea (Paläontologie), p. 840–846. *In* R. Dittler, G. Joos, E. Korschelt, G. Linek, F. Oltmanns, and K. Schaum (eds.), Handwörterbuch der Naturwissenschaften, 2nd Ed. Gustav Fisher, Jena.

SMITH, L. H. 1998a. Species level phenotypic variation in lower Paleozoic trilobites. Paleobiology, 24:17–36.

SMITH, L. H. 1998b. Asymmetry of Early Paleozoic trilobites. Lethaia, 31: 99–112.

SMITH, L. H. AND B. S. LIEBERMAN. 1999. Disparity and constraint in olenelloid trilobites and the Cambrian Radiation. Paleobiology, 25:459–470.

STITT, J. H. AND R. L. CLARK. 1984. A complete specimen of *Peachella brevispina* Palmer - an unusual olenellid trilobite (Arthropoda: Olenellida) from the lower Cambrian of California. Transactions of the San Diego Society of Natural History, 20:145–150.

SUNDBERG, F. A. 2000. Homeotic evolution in Cambrian trilobites. Paleobiology, 26:258–270.

SUNDBERG, F. A. AND L. B. MCCOLLUM. 1997. Oryctocephalids (Corynexochida: Trilobita) of the Lower-Middle Cambrian boundary interval from California and Nevada. Journal of Paleontology, 71:1065–1090.

SUNDBERG, F. A. AND L. B. MCCOLLUM. 2000. Ptychopariid trilobites of the Lower-Middle Cambrian boundary interval, Pioche Shale, southeastern Nevada. Journal of Paleontology, 74:604–630.

TASCH, P. 1952. Adaptive trend in eyeline development in the Olenellidae. Journal of Paleontology, 26:484–488.

WAGGONER, B. M. AND A. G. COLLINS. 1995. A new chondrophorine (Cnidaria, Hydrozoa) from the Cadiz Formation (Middle Cambrian) of California. Paläontologische Zeitschrift, 69:7–17.

WALCH, J. E. I. 1771. Die Naturgeschichte der Versteinerungen zur Erläuterung der Knorrischen Sammlung von Merkwürdigkeiten der Natur. Nürnberg.

WALCOTT, C. D. 1890. The fauna of the Lower Cambrian or *Olenellus* Zone, p. 509–774. *In* Tenth Annual Report of the Director, 1888–1889, United States Geological Survey.

WEBSTER, M. 2003. Olenelloid trilobites of the southern Great Basin, U.S.A., and a refinement of uppermost Dyeran biostratigraphy. Geological Society of America, Abstracts with Programs, 35(6):166.

WEBSTER, M. 2005. Intraspecific variability in Early Cambrian olenelloid trilobites: implications for biostratigraphy, regional correlation, and phylogeny. Acta Micropalaeontologica Sinica, 22(Supplement):196–197.

WEBSTER, M. In press. *Paranephrolenellus*, a new genus of Early Cambrian olenelloid trilobite. Memoirs of the Association of Australasian Palaeontologists.

WEBSTER, M. AND N. C. HUGHES. 1999. Compaction-related deformation in Cambrian olenelloid trilobites and its implications for fossil morphometry. Journal of Paleontology, 73:355–371.

WEBSTER, M. AND M. L. ZELDITCH. 2005. Evolutionary modifications of ontogeny: heterochrony and beyond. Paleobiology, 31:354–372.

WEBSTER, M., H. D. SHEETS, AND N. C. HUGHES. 2001. Allometric patterning in trilobite ontogeny: testing for heterochrony in *Nephrolenellus*, p. 105–144. *In* M. L. Zelditch (ed.), Beyond Heterochrony: The Evolution of Development. Wiley and Sons, New York.

WEBSTER, M., P. M. SADLER, M. A. KOOSER, AND E. FOWLER. 2003. Combining stratigraphic sections and museum collections to increase biostratigraphic resolution, p. 95–128. *In* P. J. Harries (ed.), High-Resolution Approaches in Stratigraphic Paleontology. Topics In Geobiology, Volume 21. Kluwer Academic Publishers, Dordrecht.

WHITE, C. A. 1874. Preliminary report upon invertebrate fossils collected by the expeditions of 1871, 1872, and 1873, with descriptions of new species. U. S. Geographic and Geologic Surveys West of the 100th Meridian Report, p. 5–27.

WHITTINGTON, H. B. 1989. Olenelloid trilobites: Type species, functional morphology and higher classification. Philosophical Transactions of the Royal Society of London, Series B, 324:111–147.

WHITTINGTON, H. B. AND S. R. A. KELLY. 1997. Morphological terms applied to Trilobita. p. 313–329. *In* R. L. Kaesler (ed.), Treatise on Invertebrate Paleontology, Pt. O, Arthropoda 1, Trilobita, Revised, Volume 1. Geological Society of America and University of Kansas Press, Lawrence.

ZELDITCH, M. L., H. D. SHEETS, AND W. L. FINK. 2003. The ontogenetic dynamics of shape disparity. Paleobiology, 29:139–156.

ZELDITCH, M. L., D. L. SWIDERSKI, H. D. SHEETS, AND W. L. FINK. 2004. Geometric Morphometrics for Biologists: A Primer. Elsevier Academic Press, Amsterdam, 443 p.

ACCEPTED 24 JANUARY 2007